의학박사 학위논문

혈관 조영술 기반 정량적 유량비를 이용한 동맥경화반의 특성 및 임상 예후 예측

Prediction of plaque characteristics and clinical outcome using angiography derived fractional flow reserve

2022년 8월

서울대학교 대학원
의학과 내과학
기유정

Ph.D. Dissertation of Medicine

Prediction of plaque characteristics and clinical outcome using angiography derived fractional flow reserve

혈관 조영술 기반 정량적 유량비를 이용한 동맥경화반의 특성 및 임상 예후 예측

August 2022

Graduate School of Medicine
Seoul National University
Internal medicine Major
You-Jeong Ki

Prediction of plaque characteristics and clinical outcome using angiography derived fractional flow reserve

지도 교수 구 본 권

이 논문을 의학박사 학위논문으로 제출함
2022년 4월

서울대학교 대학원
의학과 내과학
기유정

기유정의 의학박사 학위논문을 인준함
2022년 7월

위 원 장 _____ (인)
부위원장 _____ (인)
위 원 _____ (인)
위 원 _____ (인)
위 원 _____ (인)

Abstract

Prediction of plaque characteristics and clinical outcome using angiography derived fractional flow reserve

Graduate School of Medicine
Seoul National University
Internal medicine Major
You-Jeong Ki

Background and Objectives: Quantitative flow ratio (QFR) is novel methods for evaluating the fractional flow reserve (FFR) without the use of an invasive coronary pressure wire and pharmacologic hyperemic agent. However, the relationship between QFR and intravascular ultrasound (IVUS) data is undetermined. The aim of this study was to investigate the relationship between angiography-derived FFR and IVUS findings. Additionally, we would like to report whether the new index values obtained in QFR are helpful in predicting ischemia and the relationship between QFR and clinical outcomes in patients.

Methods: All vessels enrolled in Fractional FLow Reserve And Intravascular ultrasound-guided Intervention Strategy for Clinical OUtcomes in Patients with InteRmediate Stenosis (FLAVOUR) trial were screened and analysed for QFR. Computation of QFR was performed offline by an independent core laboratory. The

values of QFR ≤0.80 were considered hemodynamically significant, and IVUS characteristics were divided into two groups based on a QFR value of 0.80. The final QFR was the QFR value of diagnostic coronary angiography in patients without percutaneous coronary intervention (PCI) and the post PCI QFR value in patients who underwent PCI. The QFR pullback curve was analyzed, % area above the QFR pullback curve (%AAC) is defined as the percentage of the area above the QFR pullback curve (AAC) to the total area [AAC/total area × 100 (%)] . The primary comparison was per-vessel diagnostic performance as assessed by area under the receiver-operating characteristic curve (AUC) of QFR ≤0.80 versus %DS assessed by quantitative coronary angiography (QCA) for the diagnosis FFR of ≤0.80. Secondary comparison included diagnostic accuracy, sensitivity, specificity, positive predictive value, and negative predictive value for QFR and 3D QCA-derived % DS using invasive FFR as the reference standard. The predictive value of QFR data for the IVUS adverse characteristics was evaluated using the same method. The primary clinical endpoint of this study was target vessel failure (TVF) at 24 months after randomization, defined as composite of cardiac death, target vessel relation myocardial infarction, and target vessel revascularization.

Results: A total of 867 vessels were able to perform QFR analysis. Per-vessel level diagnostic accuracies of QFR and 3D QCA-derived %DS ≥50% for prediction FFR ≤0.80 were 92.7%, and 52.2%, respectively. For predicting vessels with FFR ≤0.80, QFR index was superior to the visual assessment, 2D or 3D-QCA data. AUC was higher for QFR compared with 2D QCA-derived % diameter stenosis (AUC 0.973 versus AUC 0.738). Vessels with QFR ≤0.80 had a longer lesion

length, smaller minimal lumen area and greater plaque burden compared to vessels with QFR ≥0.80. Coronary vessels with QFR ≤0.80 showed higher rates of attenuated plaque, calcified plaque, mixed plaque, plaque rupture, calcified nodule and positive remodeling and lower rates of fibrous plaque compared with those of QFR >0.80. The diagnostic accuracies of QFR for prediction IVUS anatomical stenosis and the adverse plaque characteristics were 79.0% and 59.3%, respectively. The accuracy of QFR was decreased in vessels with diffuse disease (lesion length ≥35mm). In diffuse disease, the addition of $\%AAC_{vessel}$ to contrast QFR demonstrated a tendency of improving the discrimination and reclassification of the vessels with FFR ≤0.80 (AUC from 0.898 to 0.914; NRI 0.886, p=0.011; IDI 0.053, p=0.139). The incidence of TVF at 2 years was higher in the low final QFR group (<0.92) compared with the high final QFR group (≥0.92) (low QFR vs. high QFR; 4.7% vs. 1.5%; HR: 3.21; 95% CI: 1.17-8.84; p=0.017).

Conclusions: Lower QFR value was related to IVUS defined anatomical stenosis or IVUS defined adverse plaque. The addition of contrast QFR to anatomical data had an incremental value in discriminating FFR ≤0.80, anatomical stenosis assessed by IVUS, and adverse plaque characteristics. These findings suggested that QFR can predict not only ischemic lesions but also plaque characteristics.

Keywords : Angiography derived fractional flow reserve; Quantitative flow ratio; Fractional flow reserve; Intravascular ultrasound; Adverse plaque.

Student Number : 2020-35833

List of Figures

Table of Contents

Introduction

Coronary angiography (CAG) is a traditional method for determining the severity of coronary stenosis and guiding percutaneous coronary intervention (PCI). CAG is a rather invasive procedure, a contrast medium is injected into the coronary artery, and radiographic images are taken to evaluate the lesion. Moreover, CAG is not accurate for assessing myocardial ischemia. In maximal vasodilation induced by pharmacologic agents, distal coronary pressure is directly proportional to maximum vasodilated coronary flow. Fractional flow reserve (FFR) is an invasive physiologic index and has been regarded as a gold standard tool to detect ischemia-causing stenosis. (1) Several studies have suggested that FFR-based PCI can reduce adverse clinical outcomes compared to angiography-guided PCI. (2, 3) As a result, the current guideline recommends coronary pressure-derived FFR as the standard of care for patients with intermediate-grade stenosis. (1, 4)

Although FFR is highly recommended in current guidelines, it is underused in real-world practice. There are several reasons for the low prevalence of FFR usage, including drug-induced hyperemia causing patient discomfort, prolonged procedure time, and the need for invasive pressure guidewire. (5) Quantitative flow ratio (QFR) is a novel method for evaluating the FFR without using an invasive coronary pressure wire and pharmacologic hyperemic agent. QFR is evaluated by 3-dimensional quantitative CAG and Thrombolysis In Myocardial Infarction (TIMI) frame count. Several studies have demonstrated a significant correlation between QFR and FFR, (6, 7) and evidence from a recent large clinical trial indicates that the QFR-guided PCI strategy of lesion selection improved clinical outcomes compared to angiography-guided PCI. (8) Although previous studies

have focused only on QFR values, QFR analysis provides physiological or anatomical information in addition to QFR values.

Intravascular ultrasound (IVUS) analysis provides anatomic information regarding the coronary artery lumen, vessel wall, and plaques, which can help evaluate lesion characteristics and vessel sizing. Such information is needed to evaluate the lesion morphology and perform appropriate PCI. Furthermore, after PCI, under-expansion, mal-apposition, or edge dissection can be detected by IVUS.

IVUS helps define plaque morphology and detect vulnerable plaque depending on the echo density and the presence or absence of shadowing and reverberation. (9-11) Through this information, IVUS-guided PCI improved clinical outcomes in comparison to angiography-guided PCI. (12-14)

The most frequently used invasive methods for coronary artery evaluation are IVUS and FFR. IVUS can provide accurate anatomical information, and FFR assesses the physiological significance of the vessel. Previous studies have identified relationships between FFR and IVUS parameters, including minimum lumen area, and minimum lumen diameter (MLD), but no studies have accurately demonstrated the relationship between FFR and plaque characteristics assessed by greyscale IVUS. (15, 16) Furthermore, few data are available regarding the relationship between IVUS parameters and QFR. QFR is a physiologic variable obtained by anatomical angiographic information, and it would be meaningful to evaluate how it correlates with IVUS to understand QFR.

Despite significant improvements in PCI techniques and materials, many patients are at risk of adverse clinical events related to the stent segment or residual disease. (17) In real-world practice, the completeness of the PCI is based on CAG, but it only provides information about the 2-dimensional coronary lumen. So, the prognostic value of post-PCI FFR was validated in several studies with consistent

results. (18, 19) Although procedure optimization through post-PCI FFR has been associated with a reduction of clinical events, the penetration rate of the post-PCI FFR is too low. As QFR can be obtained without pressure wire or hyperemic agent, there is a potential role for non-invasive QFRs in evaluating post-PCI physiology.

This study aimed to investigate the relationship between QFR and IVUS findings and demonstrate that other information from the QFR analysis provides further information on ischemia or plaque characteristics and the patient's prognosis. In addition, this study was to identify the ability to predict the physiology after PCI through the graph index obtained from QFR.

Materials and methods

Study design and population

The Fractional FLow Reserve And Intravascular ultrasound-guided Intervention Strategy for Clinical OUtcomes in Patients with InteRmediate Stenosis (FLAVOUR) trial was an investigator-initiated, prospective, randomized, open-label, multinational trial performed at 18 hospitals in Korea and China. The detailed study protocols, participants, and outcomes have been previously published. (20) All consecutive patients with suspected ischemic heart disease and intermediate coronary stenosis in CAG were screened for enrollment in this study. Following angiography, eligible patients with intermediate stenosis were randomized 1:1 to receive the FFR-guided PCI strategy or IVUS-guided PCI. For the FFR-guided strategy group, the criterion for revascularization was FFR ≤0.80, and for IVUS-guided strategy group, the criterion for revascularization was minimal lumen area (MLA) ≤ $3mm^2$ or $3mm^2$ < MLA ≤ $4mm^2$ and plaque burden >70%. All patients were treated with second-generation drug-eluting stents (DES). The present QFR sub-study is a post hoc analysis of the FLAVOUR trial. Vessels with suboptimal qualities of the angiographic images were excluded from this study. Other exclusion criteria included: 1) ostial lesions in major coronary arteries; 2) severe vessel overlap or tortuosity at the stenotic segments; 3) poor angiographic image quality for contour detection; 4) chronic total occlusions collateral donor vessels; 5) bifurcation lesions with Medina classification (1,1,1); 6) vessels with near total occlusion.

Quantitative coronary angiography analysis

Quantitative coronary angiography (QCA) is an imaging modality to assess the disease severity when coronary artery disease (CAD) is treated with catheter-based coronary interventions. After the calibration, the edge of the coronary vessel is gathered using an automatic edge-detection algorithm (CAAS Quantitative Coronary Angiography, Pie Medical Imaging BV, Maastricht, the Netherlands). After determining the start and end points, a path-line of the vessel is created. Then the vessel outline is drawn along the path line. (21) Generally, the following QCA values were measured: (1) minimal lumen diameter: the smallest diameter of the lumen, (2) reference diameter: the average diameter of the lumen without disease, (3) lesion length, (4) % diameter stenosis (% DS): 1 – minimal lumen diameter / reference diameter × 100 (%). Quantitative analysis of coronary angiographic images and calculation of the SYNTAX score was performed at the Seoul National University Hospital Cardiovascular Center angiographic core laboratory. Analysis was performed by an independent technician blinded to the results of FFR and IVUS.

Fractional flow reserve analysis

A 5- to 7-French coronary catheter was advanced into the ostium of the coronary artery and aortic pressure was measured through the guiding catheter. A 0.014-inch pressure monitoring wire (PressureWire X, Abbott Vascular and St. Jude Medical, St. Paul, Minnesota; or Verrata, Philips Volcano, San Diego, California) was set at zero, calibrated at the coronary ostium, advanced through the catheter, and the wire was placed at the distal part of a target vessel. (22, 23) Since the basic assumption of the FFR concept is a linear relationship between coronary blood flow and pressure, maximal hyperemia induction and minimization of microvascular resistance are essential for FFR measurements. (22, 24) Hyperemia was induced by

intravenous infusion of adenosine (140 μg/kg/min) or intracoronary nicorandil (2 mg) to induce maximal coronary blood flow, corresponding with minimal distal coronary pressure. (15) After achieving steady hyperemia, FFR was calculated by dividing the mean distal coronary pressure by the mean aortic pressure. The values of FFR ≤0.80 were considered hemodynamically significant.

Intravascular ultrasound analysis

IVUS systems have been used to obtain real-time cross-sectional images of coronary arteries. For quantitative assessment, measurements were performed on the leading edge of the boundaries, not the trailing edge. In coronary arteries, there are three layers. The most internal layer consists of the intima, atheroma, and internal elastic membrane and is echogenic compared to the lumen or media. The second layer is the media and is less echogenic than the intima; the third outer layer is adventitia (**Figure 1A, and 1B**). A discrete interface at the boundary between the media and the adventitia almost coincides with the external elastic membrane (EEM) location. The definitions of IVUS measurements were as follows (**Figure 1C**):

Proximal reference: The portion with the largest lumen within 10 mm of the proximal part of the stenosis.

Distal reference: The portion with the largest lumen within 10 mm of the distal part of the stenosis.

MLA: The area bounded by the luminal border through the center point of the lumen. MLA was measured at the narrowest part of the lesion.

Plaque plus media cross-sectional area (CSA): The EEM CSA – the lumen CSA.

Plaque burden: Plaque plus media CSA (The EEM CSA – the lumen CSA) / EEM CSA × 100 (%)

Area stenosis: (Mean reference lumen CSA – Lesion lumen CSA) / Mean reference lumen CSA × 100 (%)

Remodeling index: Vascular remodeling refers to an increase or decrease in the EEM area during atherosclerosis. The remodeling index was calculated by lesion EEM CSA divided by reference EEM CSA. If the lesion EEM is larger than the reference EEM, positive remodeling (PR) has occurred. PR was defined as a remodeling index >1.05.

Attenuated plaque (AP), fibrous plaque, calcified plaque, mixed plaque, and thrombus were evaluated for qualitative plaque assessment. (25, 26) To evaluate the characteristics of the plaque, the entire vessel, as well as the site of severe stenosis, were examined. The qualitative assessment of plaque characteristics was based on the echogenic properties of the plaque, and the degree of echogenicity of the adventitia was used as a reference. Qualitative assessment was defined as follows:

AP: Plaque with posterior attenuation without high-intensity echo reflectors involving >90° around the vessel circumference. (27)

Fibrous plaque: Plaque with an intermediate echogenicity between echo-lucent atheroma and echogenic calcified plaques.

Mixed plaque: Plaque containing two or more different acoustic subtypes (fibrocalcific, fibrofatty, etc.).

Thrombus: Thrombus is recognized as an intraluminal mass, layered, lobulated, or pedunculated morphology. (28)

Ruptured plaque: Ulcerated plaque with a cavity connected to the lumen with an overlying residual fibrous cap fragment. (29)

The ultrasound transducer was advanced over the guidewire into the distal portion of the lesion. IVUS was performed after intracoronary administration of

nitroglycerin using motorized transducer pullback (0.5 mm/s). IVUS images were analyzed in the core laboratory using computerized planimetry (EchoPlaque system, Indec Sytems Inc., Los Altos, CA) according to the validated standards. (25)

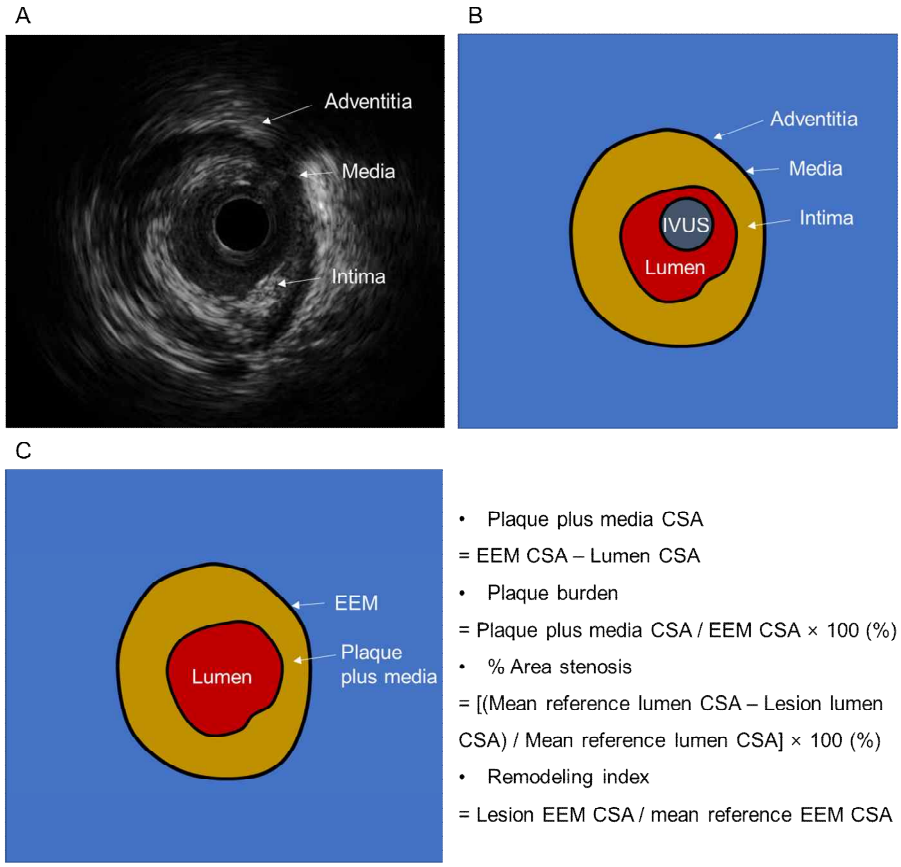

Figure 1. Scheme of IVUS measurements

(A) IVUS image, (B) schematic diagram show three-layered appearance of intima, media, and adventitia, (C) the definitions of IVUS measurements.

Abbreviations: CSA, cross-sectional area; EEM, external elastic membrane; IVUS, intravascular ultrasound.

Quantitative flow ratio analysis

QFR was retrospectively analyzed by an independent core laboratory using the software package QAngio XA 3D 1.2 (Medis Medical Imaging Systems, Leiden, the Netherlands). The core laboratory was blinded for FFR and IVUS results. End diastolic frames of two matched images separated by greater than 25° and with an acquisition time difference of ≤120 minutes were selected and used for the reconstruction of a 3-dimensional (3D) model (**Figure 2A**). The offset correction step allows the QAngio XA 3D software to know how the two images are related, by indicating a corresponding anatomical landmark. Branches or centers of local lesions can be used as anatomical indicators. After clicking an anatomical landmark in the left-hand viewport, the operator must click the same anatomical landmark in the right-hand viewport (**Figure 2B**). The second step is to define the path line and contours of the vessel segment of interest. The operator specifies the vessel segment's proximal and distal points to be analyzed (**Figure 2C**). Arterial contour was automatically detected, and a manual correction was performed if necessary. The alignment of two 2D contours in the 3D model can be improved by forcing corresponding points in the left and right-hand viewports. Reference segments are usually set automatically; there are two different ways to correct reference contours (**Figure 2D**). In the 'normal method', the operator sets the reference segment to a healthy segment with the proximal and distal parts of the lesion of interest. To correct the reference contours by a fixed proximal reference diameter method, the operator adjusts the reference diameter value at the position of the proximal marker. After the calculation of fixed QFR, the estimated contrast coronary flow was calculated using a TIMI frame-count. The operator specified the frames in which

the contrast flow enters and exits the analysis segment to calculate the flow speed (**Figure 2E**). QFR values were calculated after the 3D vessel model was reconstructed for 3D QCA analysis. The 3D QCA analysis included lesion length, %DS, area stenosis, MLD, reference diameter, and volume data. The QFR calculation was based on several principles, including 1) coronary pressure remained constant through normal epicardial coronary arteries; 2) the amount of pressure drop was determined by the stenosis geometry and the flow through the lesion; 3) the stenosis was obtainable by the deviation of the diseased lumen segment compared to the reference size; 4) coronary flow velocity was preserved in the distal part compared to the proximal flow velocity, but the mass flow decreased with the tapering of the arteries due to the presence of the lateral branches. The mean flow rate and reference vessel size from 3D QCA data can determine the mass flow rate. QFR was calculated by two approaches: (1) assuming a fixed blood flow (fQFR) (2) using a modeled hyperemic flow velocity, based on the TIMI frame count analysis without drug-induced hyperemia (cQFR) (**Figure 2F**). QFR $\leq$0.80 was considered functionally significant. Residual QFR means the new vessel QFR after the target lesion was treated by PCI.

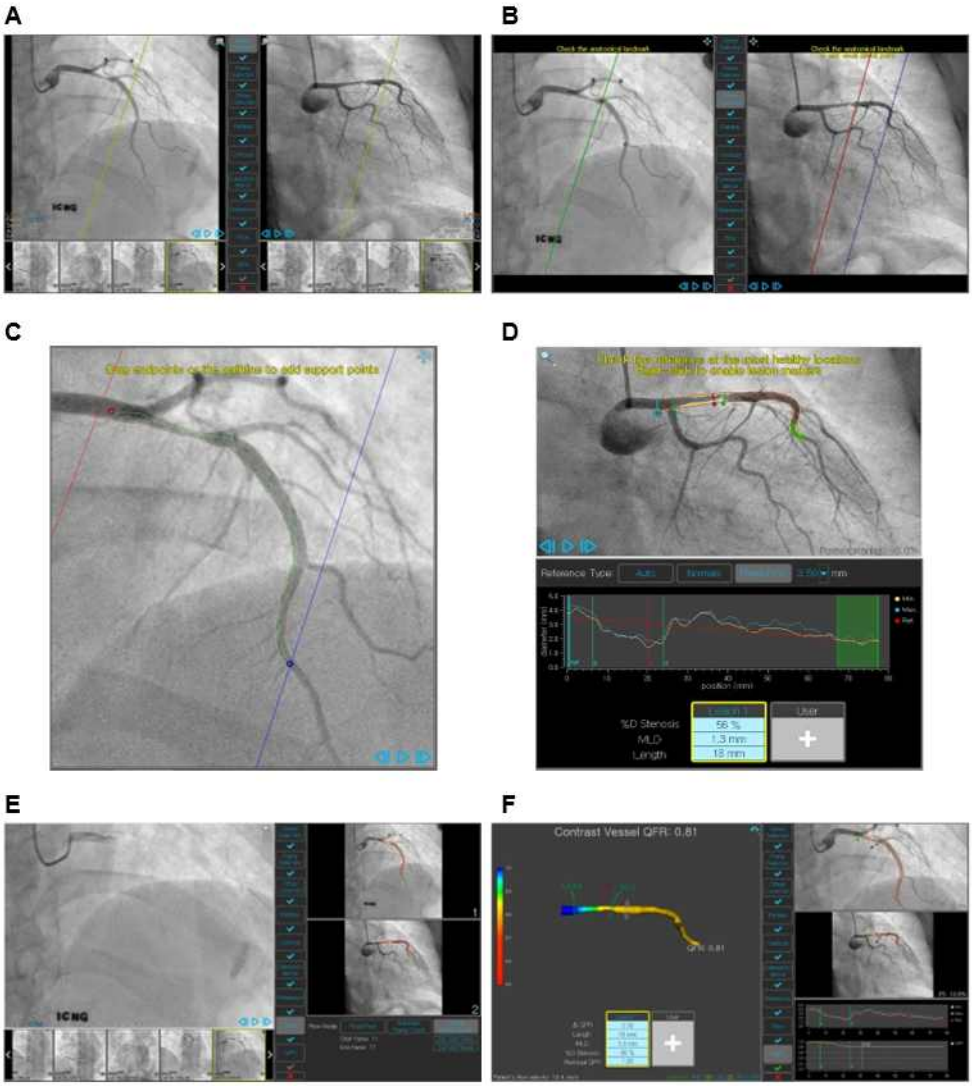

Figure 2. Steps for QFR analysis

(A) selection images, (B) offset correction, (C) pathline and contour, (D) correcting reference contours, (E) frame count, (F) QFR results.

Abbreviations: QFR, quantitative flow ratio.

Quantitative flow ratio graph analysis

QFR pullback curves were automatically derived after QFR analysis. Vessel and lesion indices were calculated using QFR tracing graphs. Using the QFR pullback curve, comprehensive physiologic indices were calculated per vessel and lesion. Per vessel indices included % area above the QFR pullback curve $(\%AAC)_{vessel}$, $angle_{vessel}$, max $angle_{vessel}$, and $slope_{vessel}$. % AAC was defined as the percentage of the area above the QFR pullback curve to the total area [Area above the QFR pullback curve/total area × 100 (%)] (**Figure 3A**). $Angle_{vessel}$ means the angle of the starting point in the QFR curve, and max $angle_{vessel}$ means the angle of the steepest part of the curve (**Figure 3B**). $Slope_{vessel}$ was the slope of a straight line from the beginning to the end of the QFR curve (**Figure 3C**). Per lesion indices included $\%AAC_{lesion}$, $angle_{lesion}$, max $angle_{lesion}$, and $slope_{lesion}$ (**Figure 3D, 3E, and Figure 3F**).

A

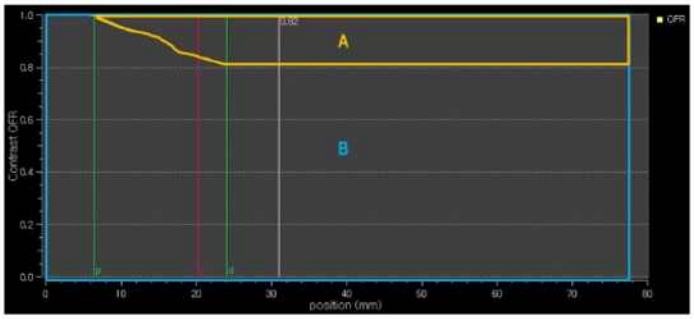

$$\%\ AAC_{vessel} = A/B\ X\ 100$$

B

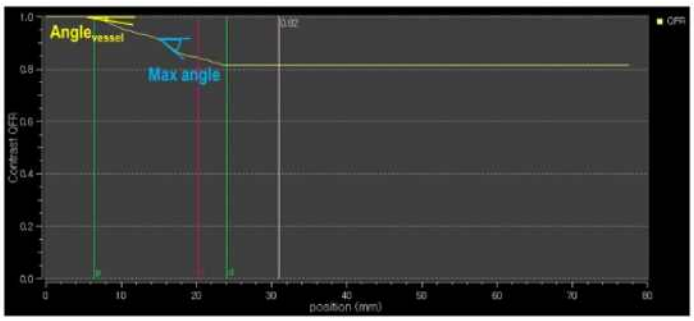

C

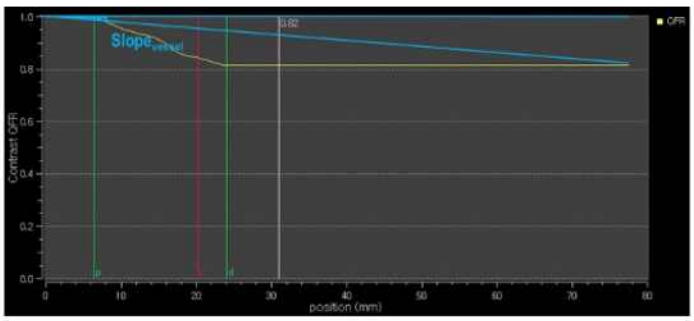

D

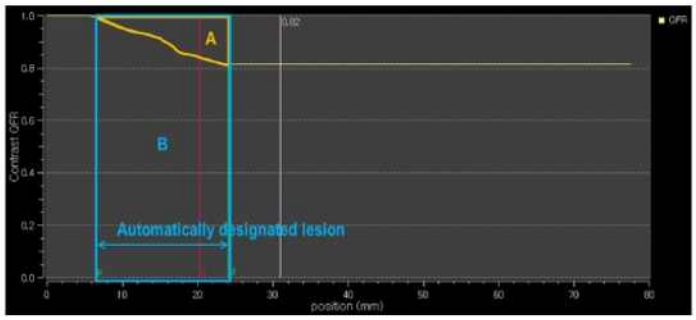

$$\%\ AAC_{lesion} = A/B\ X\ 100$$

E

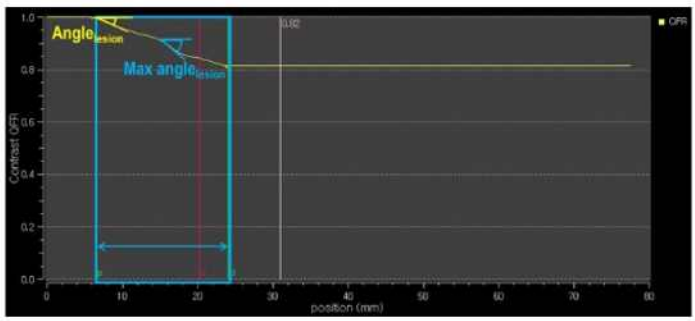

F

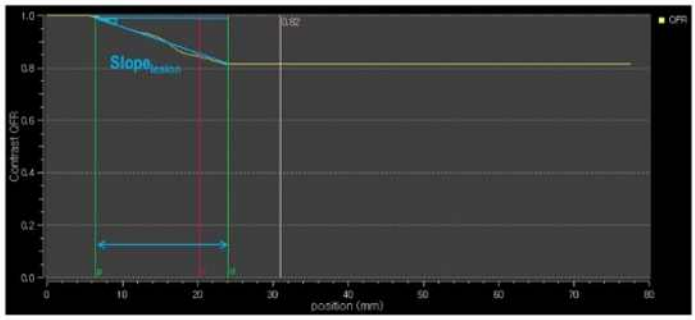

Figure 3. Description of the QFR curve index (A) % AAC, (B) angle$_{vessel}$ and max angle$_{vessel}$, (C) slope$_{vessel}$, (D) %AAC$_{lesion}$, (E) angle$_{lesion}$, and (F) slope$_{lesion}$.
Abbreviations: AAC, area above the curve, QFR, quantitative flow ratio.

Definitions and outcomes

The primary comparison was a per-vessel diagnostic performance as assessed by area under the receiver-operating characteristic curve (AUC) of QFR ≤0.80 versus %DS assessed by QCA for the diagnosis FFR of ≤0.80. The secondary comparison included diagnostic accuracy, sensitivity, specificity, positive predictive value, and negative predictive value for QFR and 3D QCA-derived % DS using invasive FFR as the reference standard. Furthermore, the predictive value of QFR data for the IVUS adverse characteristics was evaluated using the same methodology.

The primary clinical endpoint of this study was target vessel failure (TVF) at 24 months after randomization, defined as a composite of cardiac death, target vessel related myocardial infarction, and target vessel revascularization. All clinical outcomes followed the criteria provided by the Academic Research Consortium. (30)

The final QFR means the last QFR value of the target vessel. In patients without revascularization, the diagnostic angiogram's final QFR became the QFR value; in patients with revascularization, the final QFR became the post-PCI QFR value. % plaque volume (PV) / reference volume (RV) assessed by 3D QCA was calculated by PV divided by RV.

Statistical analysis

All numerical data were expressed as mean ± standard deviation for continuous variables and percentages for categorical variables. For comparison among groups, the chi-square test or Fisher's exact test was used for categorical variables and the

unpaired Student's t-test was used for continuous variables. Correlation and agreements were measured by Pearson's correlation and Bland-Altman analysis. Receiver-operating curve (ROC) analysis was performed to assess the discriminative powers of the QFR data for an FFR of ≤0.80 or adverse plaque assessed by IVUS. Diagnostic accuracy, sensitivity, specificity, positive predictive value, and negative predictive values were calculated with 95% confidence intervals (CIs). AUC was compared with the DeLong method. (31) The category free net reclassification index (NRI) and integrated discrimination improvement (IDI) analysis were performed. Multivariable logistic regression analysis was performed to identify the independent factors of an FFR ≤0.80 or adverse plaque assessed by IVUS. Variables significantly associated with an FFR of ≤0.80 or adverse plaque assessed by IVUS in univariable analyses were entered into the final model. Vessel-based multivariable analysis was performed using a generalized estimating equation approach to account for the clustered character of the data. The occurrence rate of time-dependent events was estimated using the Kaplan-Meier method, and the clinical outcomes were compared using the log-rank test. Hazard ratios (HRs) and 95% CIs were generated using Cox proportional hazard models. A two-sided p-value <0.05 was considered significant. Analyses were performed using the following statistical packages: SPSS version 23.0 (IBM SPSS Statistics, Chicago, Illinois, USA) and STATA Release 12.0 (Stata, College Station, TX, USA).

Results

Baseline clinical, angiographic, and procedural characteristics

The flow of the study is shown in **Figure 4**. In the FLAVOUR trial, 1,682 patients were successfully randomized to FFR-guided PCI (n=838) or IVUS-guided PCI (n=844). Of 1,820 vessels, 867 vessels (47.6%) in 826 patients were analyzable for QFR. The analysis failed in the other vessels for the following reasons: insufficient contrast filling (n=258); lack of auto-calibration data (n=216); two angiographic image projection angles ≤25° apart (n=157); absence of angiogram images (n=118); severe vessel overlap or tortuosity at the stenotic segments (n=107); invisible distal part of the target vessel (n=57); incomplete angiography data (n=26); DS >90% (n=8), etc. Among the QFR analyzable vessels, 452 vessels (52.1%) and 415 vessels (47.9%) were in the FFR group and IVUS strategy groups, respectively. The baseline characteristics of enrolled patients are provided in **Table 1**. The mean age of the patients was 64.9 years, 69.1% were male, and 33.2% had diabetes. The clinical diagnosis at the enrolment was acute coronary syndrome (ACS) in 30.1%. Approximately 12% of enrolled patients had a multi-vessel disease. The mean value of pre-PCI QFR was 0.84 ± 0.10. The distribution was shown in **Figure 5**.

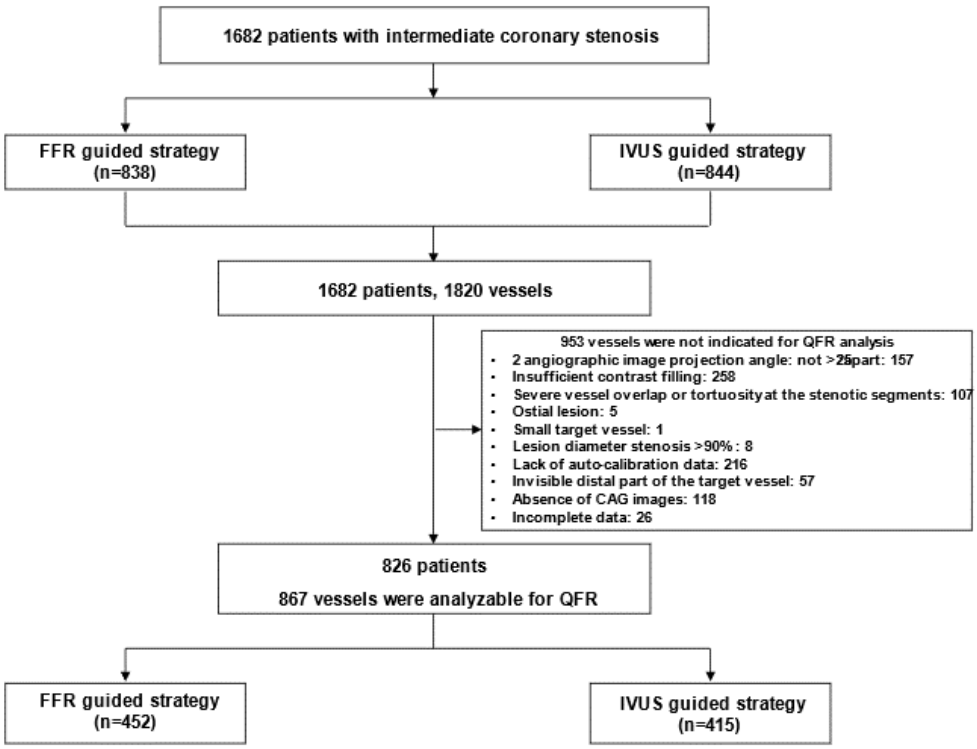

Figure 4. Study flow

Abbreviations: CAG, coronary angiography; CTO, chronic total occlusion; FFR, fractional flow reserve; IVUS, intravascular ultrasound; QFR, quantitative flow ratio .

Table 1. Baseline characteristics of the study population

Clinical characteristics	**n=826**
Age, years	64.9±9.6
Male, n (%)	571 (69.1)
Body mass index, kg/m^2	24.6±3.2
Acute coronary syndrome, n (%)	249 (30.1)
Diabetes mellitus, n (%)	274 (33.2)
Hypertension, n (%)	560 (67.8)
Dyslipidemia, n (%)	653 (79.1)
Current smoking, n (%)	146 (17.7)
Prior MI, n (%)	32 (3.9)
Prior PCI, n (%)	147 (17.8)
LV ejection fraction, %	64.2±7.6
Laboratory data	
WBC, /ul	6.6±1.9
Hemoglobin, g/dL	13.7±1.6
Creatinine, mg/dL	0.85±0.41
Total Cholesterol, mg/dL	154.5±42.5
Triglyceride, mg/dL	143±91.7
HDL-cholesterol, mg/dL	45.7±11.2
LDL-cholesterol, mg/dL	84.6±33.9
Discharge medication	
Aspirin, n (%)	643 (77.8)
P2Y$_{12}$ inhibitor, n (%)	657 (79.5)
DAPT, n (%)	515 (62.3)
Statin, n (%)	788 (95.4)
Beta blocker, n (%)	346 (41.9)
ACE inhibitor or ARB, n (%)	399 (48.3)
Calcium channel blocker, n (%)	287 (34.7)
Angiographic disease extent	
1 vessel disease, n (%)	724 (87.7)
2 vessel disease, n (%)	95 (11.5)

3 vessel disease, n (%)	7 (0.8)
SYNTAX score at baseline	8.2±5.8
SYNTAX score after PCI	5.0±4.6

Abbreviations: ACE, Angiotensin-converting enzyme; ARB, Angiotensin receptor blocker; DAPT, dual antiplatelet therapy; HDL, high-density lipoprotein; LDL, low-density lipoprotein; LV, left ventricle; MI, myocardial infarction; PCI, percutaneous coronary intervention; SYNTAX, SYNergy between percutaneous coronary intervention with TAXus and cardiac surgery; WBC, white blood cell

Data presented as mean ± standard deviation or as n (%).

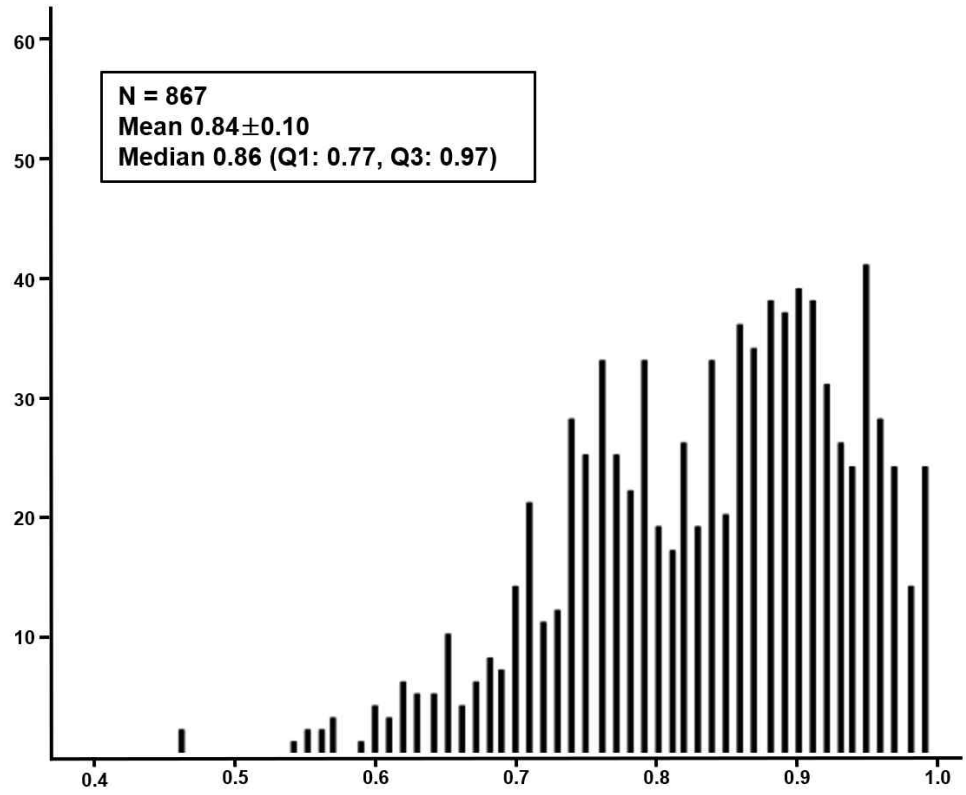

Figure 5. Distribution of pre percutaneous coronary intervention quantitative flow ratio values

Vessel and procedural characteristics of the 2 groups stratified by QFR ≤0.80 are shown in **Table 2**. The prevalence of left anterior descending artery and proximal lesions was higher in the QFR ≤0.80 group than in the QFR >0.80 group. Revascularization was performed in 92.6% of the QFR ≤0.80 group. Vessels with QFR ≤0.80 had longer lesions, smaller MLDs, and more severe stenosis in the QCA analysis. **Figure 6** shows the QFR and FFR values among %DS assessed by QCA tertiles. QFR and FFR showed a significant graded change. Both values tend to decrease gradually with increasing diameter stenosis on QCA examination.

Table 3 shows the IVUS anatomical findings, FFR results, and QFR data for each QFR group. Vessels with QFR ≤0.80 had a longer lesion length, smaller MLA, greater plaque burden, and greater volume plaque burden on IVUS examination compared to vessels with QFR >0.80. There were no significant differences in the post PCI IVUS values between the two groups, except for heavy plaque burden at minimum stent area in QFR ≤0.80.

Table 2. Baseline procedural characteristics

	Total (n=867)	QFR ≤0.80 (n=312)	QFR >0.80 (n=555)	p value
Target vessel				<0.001
Left anterior descending artery	544 (62.7%)	223 (71.5%)	321 (57.8%)	
Left circumflex artery	80 (9.2%)	24 (7.7%)	56 (10.1%)	
Right coronary artery	243 (28.0%)	65 (20.8%)	178 (32.1%)	
Location				0.001
Proximal	369 (42.6%)	160 (51.3%)	209 (37.7%)	
Mid	410 (47.3%)	125 (40.1%)	285 (51.4%)	
Distal	88 (10.1%)	27 (8.7%)	61 (11.0%)	
Patients with PCI	367 (42.3%)	289 (92.6%)	78 (14.1%)	<0.001
Patients with stent	363 (41.9%)	288 (92.3%)	75 (13.5%)	<0.001
Patients with balloon	4 (0.5%)	1 (0.3%)	3 (0.5%)	1.000
Total stent number	0.5±0.6	1.1±0.5	0.2±0.4	<0.001
Total stent length, mm	30.8±13.5	31.4±13.9	28.4±11.7	0.083
Diameter of stents, mm	3.2±0.4	3.2±0.4	3.2±0.4	0.230
Quantitative coronary angiography				
Lesion length	19.6±10.1	23.1±11.7	17.6±8.6	<0.001
Minimal lumen diameter	1.3±0.4	1.1±0.3	1.4±0.4	<0.001
Reference diameter	3.0±0.5	2.9±0.5	3.0±0.5	<0.001
% Diameter stenosis	55.8±10.1	61.9±8.8	52.4±9.2	<0.001

Abbreviations: PCI, percutaneous coronary intervention; QFR, quantitative flow ratio.

Data presented as mean ± standard deviation or as n (%).

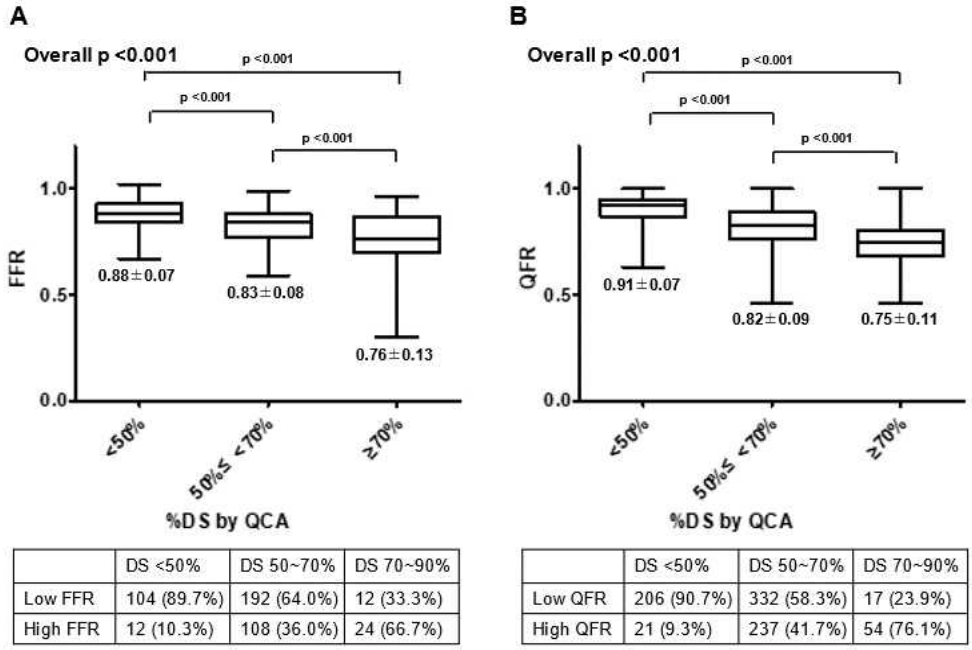

	DS <50%	DS 50~70%	DS 70~90%
Low FFR	104 (89.7%)	192 (64.0%)	12 (33.3%)
High FFR	12 (10.3%)	108 (36.0%)	24 (66.7%)

	DS <50%	DS 50~70%	DS 70~90%
Low QFR	206 (90.7%)	332 (58.3%)	17 (23.9%)
High QFR	21 (9.3%)	237 (41.7%)	54 (76.1%)

Figure 6. Pre PCI physiology in various angiographic subgroups

Abbreviations: DS, diameter stenosis; FFR, fractional flow reserve; IVUS, intravascular ultrasound; QCA, quantitative coronary angiography; QFR, quantitative flow ratio.

Table 3. IVUS, FFR, and QFR characteristics of the studied vessels

	Total	QFR ≤0.80	QFR >0.8	p value
IVUS findings (n=409)				
Lesion length, mm	21.9±11.2	25.6±13.1	19.6±9.1	<0.001
Minimum lumen area, mm^2	3.5±1.2	2.7±0.7	4.0±1.2	<0.001
Plaque burden, %	70.1±9.6	75.9±6.9	66.5±9.3	<0.001
Total plaque volume (l)	70.9±8.7	75.7±7.5	68.0±8.1	<0.001
Volume plaque burden (l)	0.6±0.1	0.6±0.1	0.5±0.1	<0.001
Mean lumen area, mm^2 (l)	6.1±1.7	5.5±1.5	6.4±1.8	<0.001
Mean vessel area, mm^2 (l)	13.8±3.9	13.3±3.7	14.2±4.0	0.027
Mean plaque area, mm^2 (l)	7.8±2.6	7.8±2.6	7.7±2.7	0.783
Distal reference lumen area, mm^2	7.6±2.8	7.0±2.7	8.0±2.9	<0.001
MSA, mm^2	7.1±2.2	7.0±2.1	7.2±2.4	0.737
Minimum stent diameter at MSA, mm	2.5±0.4	2.5±0.4	2.6±0.4	0.052
Maximum stent diameter at MSA, mm	3.1±0.4	3.0±0.4	3.1±0.4	0.116
Vessel area at MSA, mm^2	13.8±4.2	13.7±4.2	14.0±4.3	0.648
Plaque burden at MSA, %	53.1±9.6	54.1±9.6	50.9±9.3	0.036
Plaque burden at proximal stent edge, %	40.5±11.6	40.9±11.9	39.7±10.8	0.496
Plaque burden at distal stent edge, %	35.8±12.7	34.9±12.5	37.8±12.9	0.154
FFR data (n=452)				
FFR pre	0.84±0.09	0.75±0.07	0.88±0.05	<0.001
Delta FFR pre	0.09±0.07	0.14±0.08	0.06±0.04	<0.001
FFR post	0.88±0.05	0.88±0.05	0.90±0.04	0.294
Delta FFR post	0.04±0.04	0.04±0.04	0.03±0.02	0.360
QFR data (n=867)				
Fixed QFR	0.84±0.10	0.73±0.07	0.89±0.06	<0.001

Contrast QFR	0.84±0.10	0.73±0.06	0.90±0.05	<0.001
Contrast flow velocity, cm/s	18.3±7.9	20.4±7.4	17.1±7.9	<0.001
Fixed flow velocity, cm/s	33.6±4.7	33.3±5.2	33.8±4.3	0.139
Post PCI QFR	0.95±0.06	0.94±0.06	0.98±0.02	0.002
Final QFR	0.91±0.06	0.91±0.09	0.91±0.05	0.887

Data presented as mean ± standard deviation or as n (%).

Abbreviations: FFR, fractional flow reserve; IVUS, intravascular ultrasound; MSA, minimum stent area; PCI, percutaneous coronary intervention; QFR, quantitative flow ratio.

The results of the FFR values were also well correlated to QFR groups. Vessels with QFR ≤0.80 had significantly lower FFR values and higher delta FFR values than those with QFR >0.80. However, post FFR and post delta FFR were similar between the two groups. The vessels with QFR ≤0.80 had lower fixed QFR, lower contrast QFR, and higher contrast flow velocity than those with QFR >0.80. Although post PCI QFR was lower in vessels with ischemia, the final QFR was similar to those with QFR >0.80. **Figure 7** shows the correlation and agreement between QFR and FFR values. There was a good correlation (Pearson's correlation coefficient: 0.75; p <0.001) and agreement (mean difference: +0.002, limits of agreement: -0.33 to 0.22), with a slight underestimation of QFR compared with FFR. The diagnostic performance of QFR ≤0.80 and 3D QCA-derived %DS ≥50% for predicting FFR ≤0.80 is shown in **Table 4**. The diagnostic accuracy of QFR ≤0.80 for predicting FFR ≤0.80 was 92.7%, whereas that of 3D QCA-derived %DS ≥50% for predicting FFR ≤0.80 was 52.2%. The sensitivity and specificity of QFR ≤0.80 for predicting FFR ≤0.80 were 91.7% and 93.2%, respectively. QFR had false discovery and false omission rates of 13.7% and 4.0%, respectively. The sensitivity and specificity of 3D QCA-derived %DS ≥50% for predicting FFR ≤0.80 were 91.7% and 33.8%, respectively. 3D QCA-derived %DS had false discovery and false omission rates of 67.7% and 10.3%, respectively.

The results of the QFR and 3D QCA values of culprit lesion data are described in **Table 5**. Regarding 3D QCA-derived culprit lesion analysis, the low QFR group was associated with a longer lesion length, severely stenotic lesion (%DS and % area stenosis), and smaller diameter than the high QFR group. The volume data

was also automatically calculated; PV and RV were higher in culprit lesions of vessels with QFR ≤0.80. Percent PV/RV was higher in culprit lesions of vessels with QFR ≤0.80 than in those with QFR >0.80. Delta fixed QFR and delta contrast QFR values were higher in the low QFR group. Since delta fixed QFR and delta contrast QFR values were higher, the residual QFR values were lower in the low QFR group.

Independent predictors for FFR ≤0.80

Compared to non-ischemia-casing lesions, coronary artery lesions that caused ischemia consisted of proximal lesions, low QFR values (QFR ≤0.80), severe stenosis, long lesions, high %PV/RV, and high delta contrast QFR. Multivariable analysis demonstrated that only low QFR was independently associated with FFR ≤0.80 (**Table 6**).

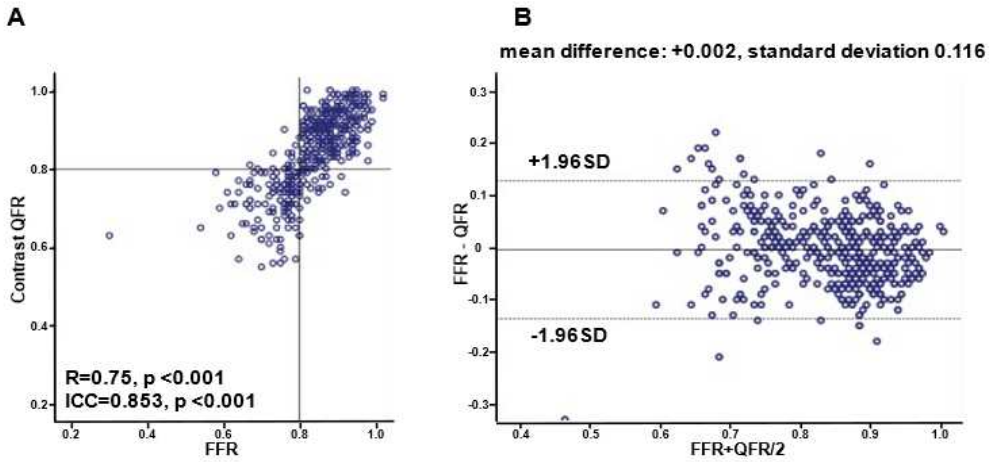

Figure 7. (A) Correlation between FFR and QFR (R^2=0.563, R=0.750, B: 0.859, SE: 0.036; p <0.001), (B) Bland-Altman plot of FFR and QFR on a per-vessel basis (mean difference, +0.002; standard deviation 0.116, p=0.016, upper limit of agreement = 0.22, lower limit of agreement = -0.33).

Abbreviations: FFR, fractional flow reserve; ICC, interclass correlation; QFR, quantitative flow ratio; SD, standard deviation; SE, standard error.

Table 4. Comparison of diagnostic performance and discriminant function of QFR, and QCA-derived % diameter stenosis with Fractional Flow Reserve ≤0.80 as a reference standard

	QFR ≤0.80	3D QCA-derived %DS ≥50%
True positive	132 (29.2)	132 (29.2)
True negative	287 (63.5)	104 (23.0)
False positive	21 (4.6)	204 (45.1)
False negative	12 (2.7)	12 (2.7)
Accuracy, %	92.7 (89.9-94.9)	52.2 (47.5-56.9)
Sensitivity, %	91.7 (85.9-95.6)	91.7 (85.9-95.6)
Specificity, %	93.2 (89.8-95.7)	33.8 (28.5-39.4)
Positive predictive value, %	86.3 (80.6-90.5)	32.3 (37.1-41.5)
Negative predictive value, %	96.0 (93.3-97.6)	89.7 (83.1-93.8)
Positive likelihood ratio	13.4 (8.9-20.4)	1.4 (1.3-1.5)
Negative likelihood ratio	0.09 (0.05-0.15)	0.25 (0.14-0.43)

Abbreviations: DS, diameter stenosis; QCA, quantitative coronary angiography; QFR, quantitative flow ratio.

Table 5. 3D QCA and QFR values of culprit lesion stratified by the cutoff value of pre QFR value at the vessel level

	Total (n=867)	QFR ≤0.80 (n=312)	QFR >0.80 (n=555)	p value
Anatomical culprit lesion				
Lesion length, mm	21.9±11.5	26.4±13.2	19.3±9.5	<0.001
Diameter stenosis, %	46.5±10.1	54.1±8.7	42.2±8.2	<0.001
Area stenosis, %	63.2±12.5	71.6±9.9	58.4±11.2	<0.001
Minimum lumen diameter, mm	1.5±0.4	1.3±0.3	1.7±0.4	<0.001
Reference diameter, mm	2.9±0.4	2.8±0.4	2.9±0.4	0.028
Area at minimum lumen diameter, mm^2	2.4±1.5	1.8±0.8	2.8±1.7	<0.001
Reference area, mm^2	6.5±2.1	6.3±2.0	6.6±2.2	0.023
Reference volume, mm^2	142.0±86.9	164.7±97.0	129.1±77.8	<0.001
Plaque volume, mm^2	50.6±34.3	65.7±39.9	42.0±27.2	<0.001
Lumen volume, mm^2	92.9±57.5	101.8±61.5	87.8±54.5	0.001
% Plaque volume / reference volume	34.9±8.0	39.6±7.3	32.2±7.1	<0.001
Delta contrast QFR	0.13±0.09	0.21±0.08	0.08±0.05	<0.001
Delta fixed QFR	0.13±0.09	0.21±0.08	0.09±0.05	<0.001
Residual contrast QFR	0.96±0.06	0.94±0.07	0.98±0.05	<0.001
Residual fixed QFR	0.97±0.06	0.94±0.06	0.98±0.05	<0.001

Data presented as mean ± standard deviation or as n (%).

Abbreviations: QCA, quantitative coronary angiography; QFR, quantitative flow ratio.

Table 6. Independent predictors for FFR ≤0.80

	Univariable analysis OR (95% CI)	p value	Multivariable analysis OR (95% CI)	p value
Proximal lesion	2.074 (1.386-3.103)	<0.001	-	-
QFR ≤0.80	150.333 (71.826-314.649)	<0.001	63.174 (24.03-166.09)	<0.001
% Diameter stenosis assessed by QCA	5.608 (2.968-10.597)	<0.001	-	-
Lesion length assessed by 3D QCA	1.063 (1.042-1.084)	<0.001	-	-
%PV/RV assessed by 3D QCA	1.142 (1.104-1.181)	<0.001	-	-
Delta contrast QFR	6.227E10 (677E8-5727E12)	<0.001	-	-

Abbreviations: CI, confidence interval; FFR, fractional flow reserve; OR, odds ratio; PV, plaque volume; RV, reference volume; QCA, quantitative coronary angiography; QFR, quantitative flow ratio.

Relationship between IVUS findings and QFR

Table 7 shows the IVUS findings stratified by the QFR value. The rate of IVUS MLA ≤3mm^2, IVUS MLA ≤4mm^2, and plaque burden ≥70% were significantly higher in vessels with QFR ≤0.80. When MLA ≤3mm^2 or (MLA≤4mm^2 & PB ≥70%) were used as IVUS criteria for revascularization, the rate of meeting the IVUS criteria for revascularization was significantly higher in vessels with QFR ≤0.80. One-third of vessels with anatomical stenosis had a QFR >0.80, and 6.4% of vessels without anatomical stenosis had a QFR ≤0.80. Plaque characteristics were well discriminated in each QFR group. Coronary vessels with QFR ≤0.80 showed higher rates of AP, calcified plaque, mixed plaque, plaque rupture, calcified nodule and PR and lower rates of fibrous plaque than those of QFR >0.80 (**Table 7**). When adverse plaques were defined as AP, PR, or rupture, vessels with lower QFR values tended to have adverse plaques. **Figure 8** shows the anatomical or morphological IVUS findings among QFR tertiles. QFR showed a significant graded change, except for the rate of PR. Depending on the QFR value, anatomical differences in IVUS and plaque characteristics can be identified.

Table 7. IVUS findings stratified by the cutoff value of pre QFR value at vessel level

	Total (n=409)	QFR ≤0.80 (n=157)	QFR >0.80 (n=252)	p value
IVUS anatomical stenosis* (+)	223/409 (54.5%)	147/157 (93.6%)	76/252 (30.2%)	<0.001
IVUS anatomical stenosis (-)	186/409 (45.5%)	10/157 (6.4%)	176/252 (69.8%)	
IVUS MLA ≤3mm²	154/409 (37.7%)	111/157 (70.7%)	43/252 (17.1%)	<0.001
IVUS MLA ≤4mm²	299/409 (73.1%)	155/157 (98.7%)	144/252 (57.1%)	<0.001
Plaque burden ≥70%	231/408 (56.6%)	131/156 (84.0%)	100/252 (39.7%)	<0.001
IVUS plaque characteristics (n=381)				
Attenuated plaque	216 (56.5%)	100 (68.5%)	116 (49.2%)	<0.001
Calcified plaque	260 (68.2%)	109 (74.7%)	151 (64.3%)	0.034
Mixed plaque	158 (41.5%)	77 (52.7%)	81 (34.5%)	<0.001
Fibrous plaque	59 (15.5%)	13 (8.9%)	46 (19.6%)	0.005
Plaque rupture	35 (9.2%)	29 (19.9%)	6 (2.6%)	<0.001
Thrombus	5 (1.3%)	3 (2.1%)	2 (0.9%)	0.376
Calcified nodule	82 (21.5%)	41 (28.1%)	41 (17.4%)	0.014
Remodeling index	0.81±0.18	0.82±0.20	0.81±0.16	0.496
PR	34 (8.8%)	20 (13.2%)	14 (6.0%)	0.015
Attenuated plaque or PR	233 (60.8%)	109 (73.6%)	124 (52.8%)	<0.001
Attenuated plaque and PR	17 (4.4%)	11 (7.3%)	6 (2.5%)	0.025
Attenuated plaque or PR or rupture	244 (63.7%)	118 (79.7%)	126 (53.6%)	<0.001
Attenuated plaque and PR and rupture	1 (0.3%)	1 (0.7%)	0 (0%)	0.389

Data presented as mean ± standard deviation or as n (%).

*IVUS anatomical stenosis: MLA ≤3mm^2 OR (MLA≤4mm^2 & PB ≥70%)

Abbreviations: IVUS, intravascular ultrasound; MLA, minimum lumen area; PR, positive remodeling; QFR, quantitative flow ratio.

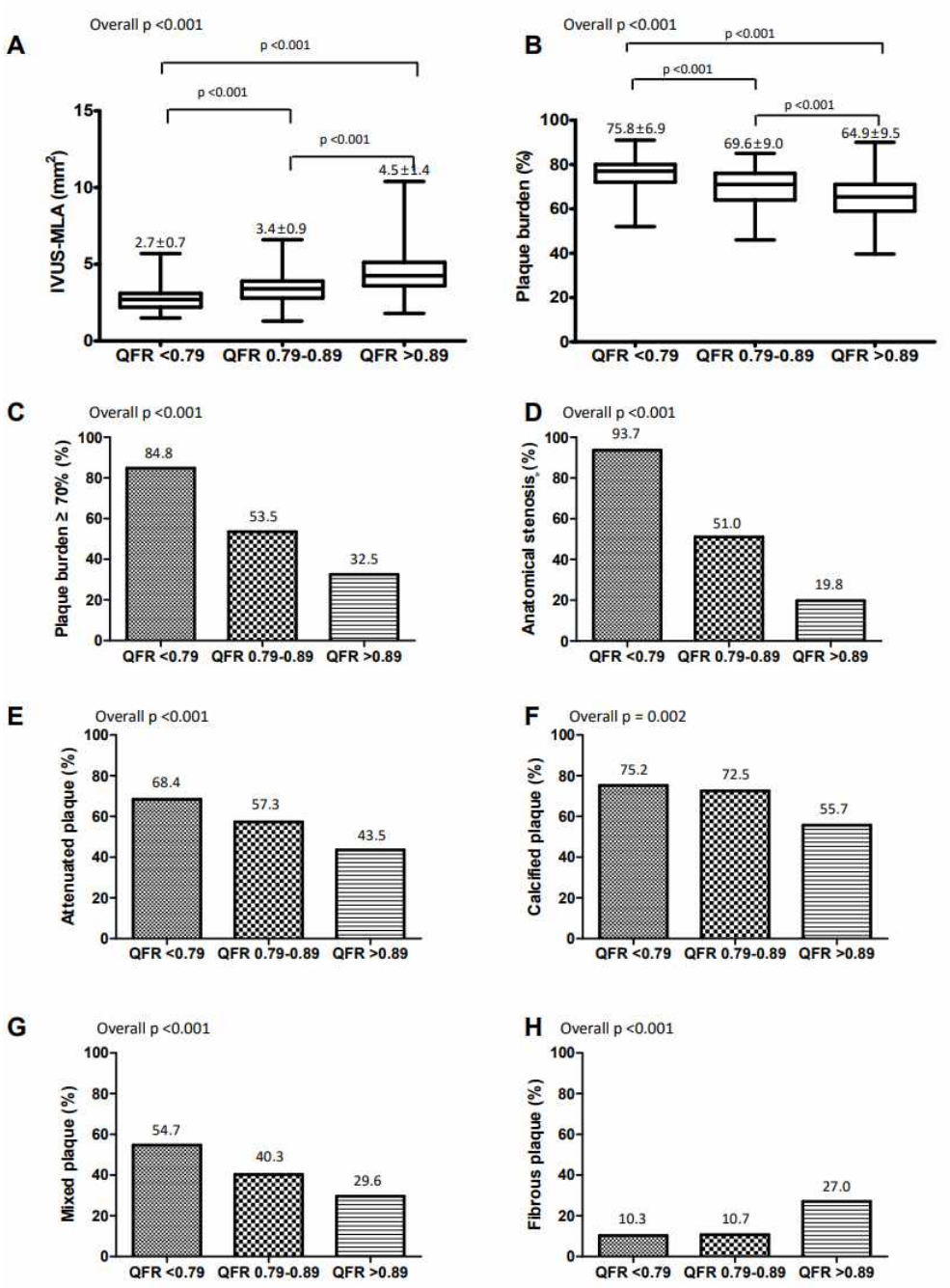
A
Overall p <0.001
p <0.001
p <0.001
p <0.001
IVUS-MLA (mm²)
2.7±0.7
3.4±0.9
4.5±1.4
QFR <0.79
QFR 0.79-0.89
QFR >0.89
B
Overall p <0.001
p <0.001
p <0.001
p <0.001
Plaque burden (%)
75.8±6.9
69.6±9.0
64.9±9.5
QFR <0.79
QFR 0.79-0.89
QFR >0.89
C
Overall p <0.001
Plaque burden ≥ 70% (%)
84.8
53.5
32.5
QFR <0.79
QFR 0.79-0.89
QFR >0.89
D
Overall p <0.001
Anatomical stenosis (%)
93.7
51.0
19.8
QFR <0.79
QFR 0.79-0.89
QFR >0.89
E
Overall p <0.001
Attenuated plaque (%)
68.4
57.3
43.5
QFR <0.79
QFR 0.79-0.89
QFR >0.89
F
Overall p = 0.002
Calcified plaque (%)
75.2
72.5
55.7
QFR <0.79
QFR 0.79-0.89
QFR >0.89
G
Overall p <0.001
Mixed plaque (%)
54.7
40.3
29.6
QFR <0.79
QFR 0.79-0.89
QFR >0.89
H
Overall p <0.001
Fibrous plaque (%)
10.3
10.7
27.0
QFR <0.79
QFR 0.79-0.89
QFR >0.89

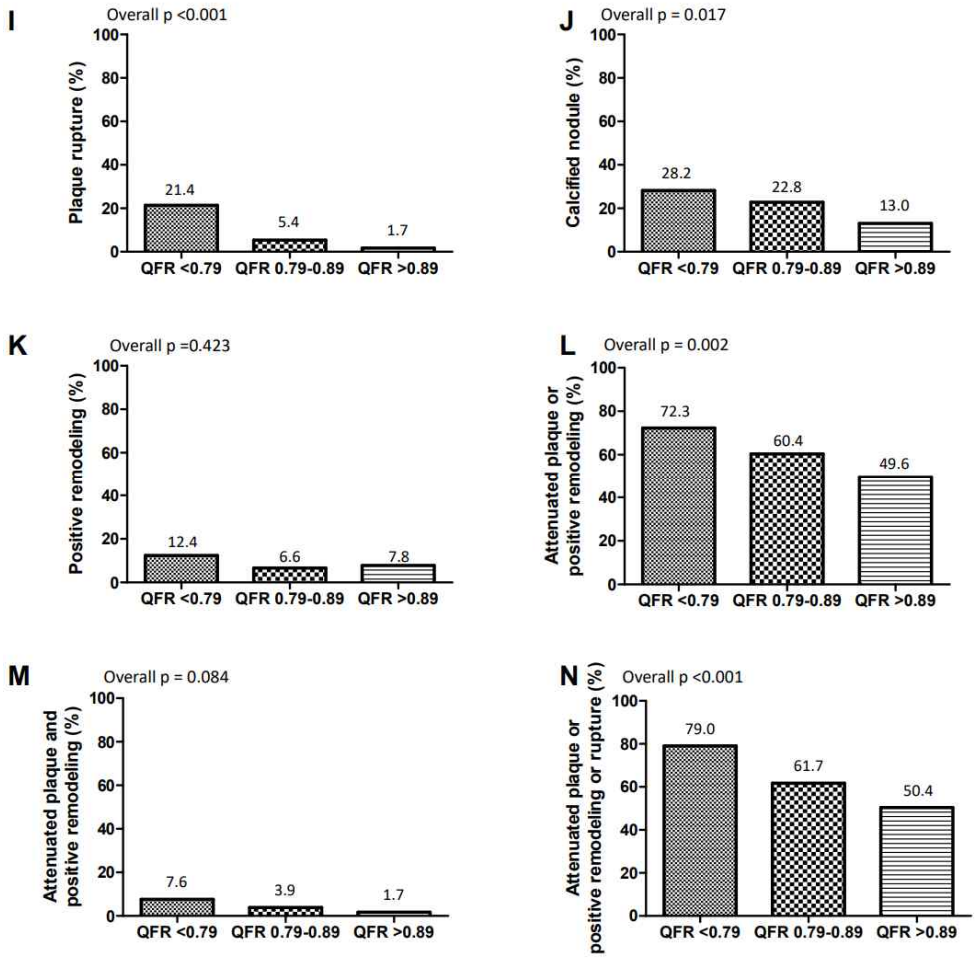

Figure 8. IVUS findings stratified by the QFR value

Abbreviations: IVUS, intravascular ultrasound; MLA, minimum lumen area; QFR, quantitative flow ratio.

With 3D QCA, the MLD-derived area is automatically calculated. Comparing this to the MLA assessed by IVUS showed a good correlation (Pearson's correlation coefficient: 0.62; p <0.001, **Figure 9**). The distribution of the QFR value and the plaque burden obtained from IVUS was similar to the QFR distribution and the % PV/RV assessed from 3D QCA (**Figure 10**). This trend was similar to the distribution of MLA (obtained from IVUS) or MLD-derived area (assessed by 3D QCA) and QFR.

Table 8 shows the diagnostic abilities of QFR ≤0.80 to predict adverse plaques on IVUS. The sensitivity and specificity of QFR ≤0.80 for predicting IVUS anatomical stenosis were 65.9% and 94.6%, respectively. QFR had 6.4% and a 30.2% false discovery and omission rates, respectively. The diagnostic accuracy of QFR ≤0.80 for predicting IVUS anatomical stenosis [MLA ≤3mm^2 OR (MLA≤4mm^2 & PB ≥70%)] and adverse plaque characteristics (AP or PR or rupture) were 79.0% and 59.3%, respectively. The QFR diagnostic accuracy was better for anatomical stenosis than for plaque characteristics.

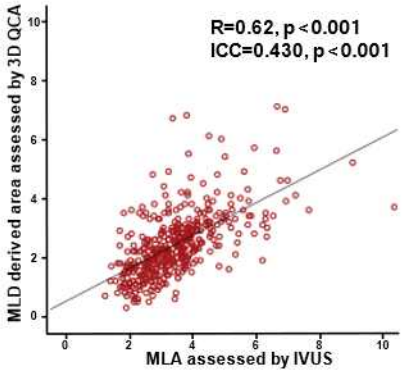

Figure 9. Correlation between 3D QCA- and IVUS- derived area

Abbreviations: ICC, intraclass correlation coefficient; IVUS, intravascular ultrasound; MLA, minimum lumen area; MLD, minimum lumen diameter; QCA, quantitative coronary angiography.

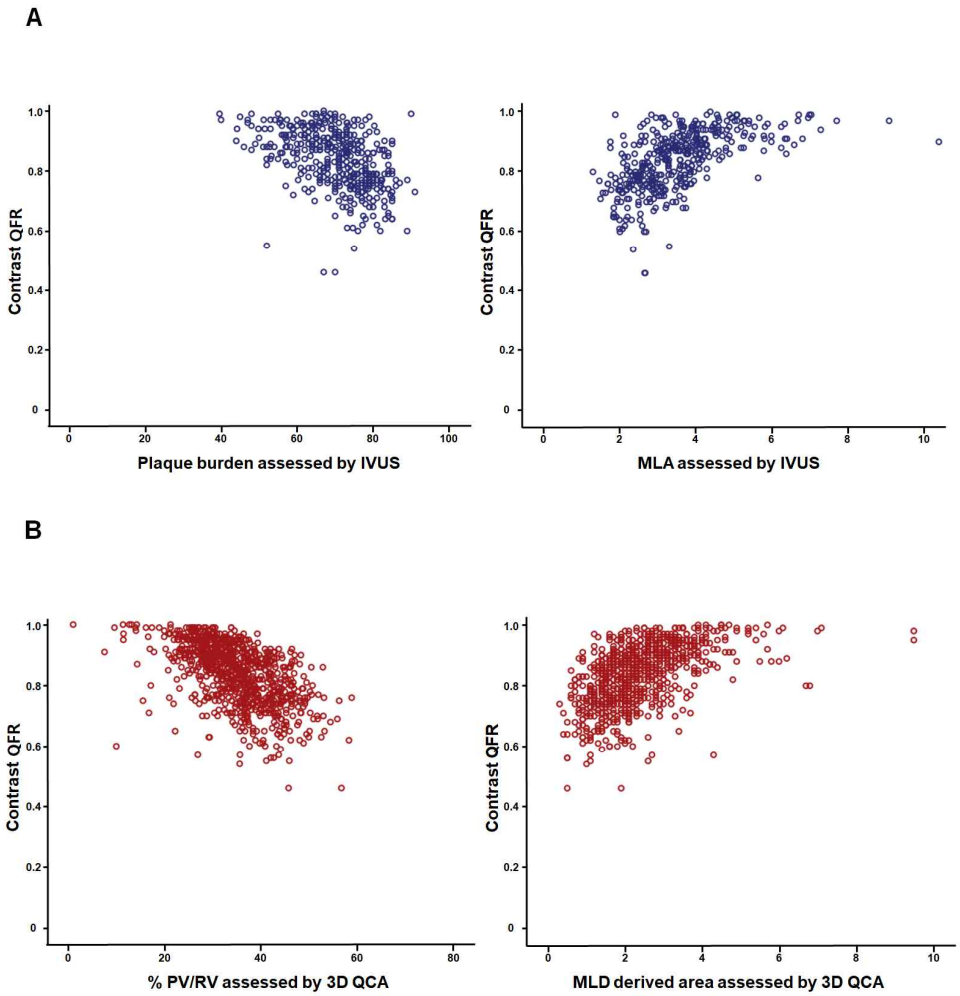

Figure 10. Distribution between IVUS-derived or 3D QCA-derived index and QFR

Abbreviations: IVUS, intravascular ultrasound; MLA, minimum lumen area; MLD, minimum lumen diameter; PV, plaque volume; QCA, quantitative coronary angiography; QFR, quantitative flow ratio; RV, reference volume.

Table 8. Diagnostic abilities of QFR ≤0.80 to predict adverse plaques on IVUS

	IVUS anatomical stenosis*	Attenuated plaque or PR	Attenuated plaque and PR	Attenuated plaque or PR or rupture
True positive	147 (35.9)	109 (28.4)	11 (2.8)	118 (30.8)
True negative	176 (43.1)	111 (29.0)	230 (59.6)	109 (28.5)
False positive	10 (2.4)	39 (10.2)	139 (36.0)	30 (7.8)
False negative	76 (18.6)	124 (32.4)	6 (1.6)	126 (32.9)
Accuracy, %	79.0 (74.7-82.8)	57.4 (52.3-62.5)	62.4 (57.4-67.3)	59.3 (54.2-64.2)
Sensitivity, %	65.9 (59.3-72.1)	46.8 (40.2-53.4)	64.7 (38.3-85.8)	48.4 (41.9-54.8)
Specificity, %	94.6 (90.3-97.4)	74.0 (66.2-80.8)	62.3 (57.2-67.3)	78.4 (70.7-84.9)
Positive predictive value, %	93.6 (88.9-96.4)	73.7 (67.4-79.1)	7.3 (5.2-10.3)	79.7 (73.6-84.7)
Negative predictive value, %	69.8 (65.8-73.6)	47.2 (43.4-51.1)	97.5 (95.3-98.7)	46.4 (42.7-50.1)
Positive likelihood ratio	12.3 (6.7-22.6)	1.8 (1.3-2.4)	1.7 (1.2-2.5)	79.7 (73.6-84.7)
Negative likelihood ratio	0.36 (0.30-0.43)	0.7 (0.6-0.8)	0.6 (0.3-1.1)	46.4 (42.7-50.1)

*IVUS anatomical stenosis: MLA ≤3mm^2 OR (MLA≤4mm^2 & PB ≥70%)

Abbreviations: IVUS, intravascular ultrasound; PR, positive remodeling; QFR, quantitative flow ratio.

Independent predictors for high-risk plaque

When adverse plaques were defined as AP, PR, or rupture, lesions with adverse plaques had low QFR, severe %DS, small MLA, severe plaque burden by IVUS, high maximum angle in QFR curve, high lesion %AAC, high lesion slope, and %PV/RV assessed by 3D QCA. In multivariable analysis, QFR ≤0.80 and plaque burden assessed by IVUS were associated with FFR ≤0.80 (**Table 9**).

Clinical outcomes

During the 24-month follow-up period, TVF occurred in 6 and 21 patients in the low QFR and high QFR groups, respectively (low vs. high: 1.9% vs. 3.8%; HR: 0.50; 95% CI: 0.20–1.25; p=0.362). Most vessels (92.6%) with QFR ≤0.80 underwent revascularization, and the incidence of TVF was lower in vessels with QFR ≤0.80 than in those with QFR >0.80. Clinical outcomes were different depending on the final QFR value, which is the final QFR value. The incidence of TVF at 2 years was higher in the low final QFR group (<0.92) compared with the high final QFR group (≥0.92) (low vs. high: 4.7% vs. 1.5%; HR: 3.21; 95% CI: 1.17–8.84; p=0.017) (**Figure 11**).

Table 9. Independent predictors for the high-risk plaque (attenuation plaque, positive remodeling, or rupture)

	Univariable analysis OR (95% CI)	p value	Multivariable analysis OR (95% CI)	p value
QFR ≤0.80	3.403 (2.114-5.476)	<0.001	3.357 (1.632-6.904)	0.001
% Diameter stenosis assessed by QCA	1.035 (1.013-1.057)	0.002	-	-
MLA assessed by IVUS	0.783 (0.660-0.929)	0.005	-	-
Plaque burden assessed by IVUS	1.063 (1.039-1.089)	<0.001	1.045 (1.017-1.074)	0.002
Vessel max angle	1.020 (1.007-1.032)	0.002	-	-
Lesion %AAC	1.063 (1.022-1.106)	0.002	-	-
Lesion slope	1.028 (1.006-1.050)	0.014	-	-
%PV/RV assessed by 3D QCA	1.046 (1.017-1.075)	0.002	-	-

Abbreviations: AAC, area above the curve; CI, confidence interval; IVUS, intravascular ultrasound; MLA, minimal lumen area; OR, odds ratio; PV, plaque volume; QCA, quantitative coronary angiography; QFR, quantitative flow ratio; RV, reference volume.

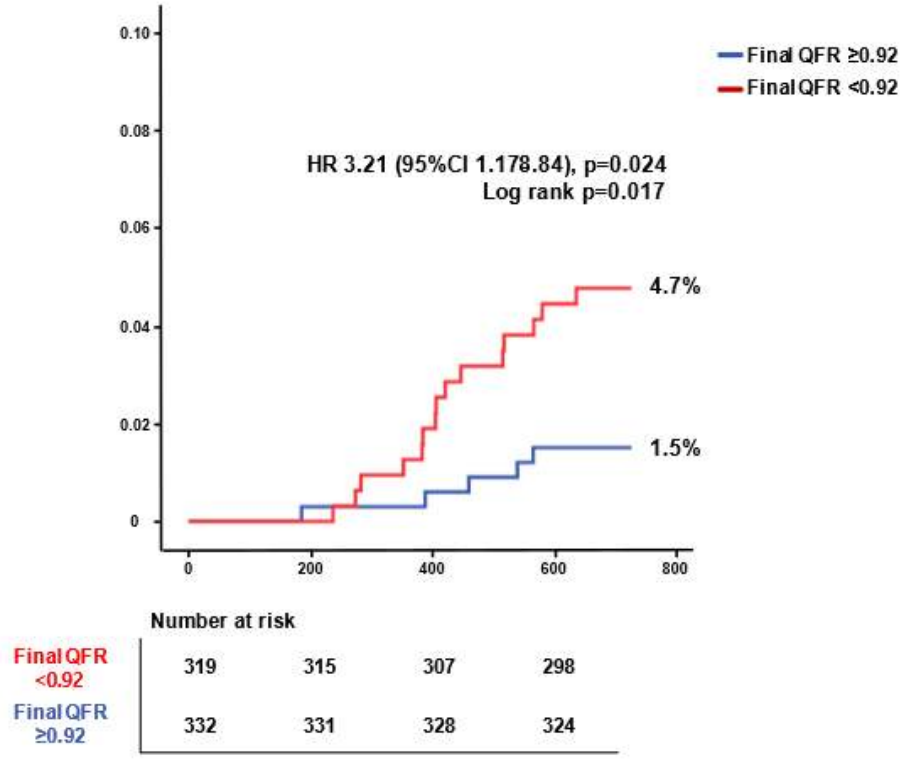

Figure 11. Kaplan-Meier curves for 2-year TVF in the final QFR <0.92 group versus final QFR ≥0.92 group

Abbreviations: CI, confidence interval; HR, hazard ratio; QFR, quantitative flow ratio; TVF, target vessel failure.

Incremental value of QFR

The addition of contrast QFR to % DS assessed by 2D QCA or % DS assessed by 3D QCA significantly improved the discrimination of the vessel with FFR ≤0.80 (AUC: from 0.742 to 0.973; NRI: 1.663, p <0.001; IDI: 0.585, p <0.001 in %DS assessed by 2D QCA and AUC: from 0.828 to 0.973; NRI: 1.561, p <0.001; IDI: 0.433, p <0.001 in % DS by 3D QCA) (**Table 10**). **Figure 12** shows ROC curves for QFR, 2D QCA-derived %DS, 3D QCA-derived area stenosis, and visual estimation for predicting FFR ≤0.80. The AUC of the QFR value was 0.973. For predicting vessels with FFR ≤0.80, the 3D QCA-derived index was superior to the visual assessment or 2D QCA data. However, QFR was the most effective value.

Furthermore, the contrast QFR also improved the discrimination of anatomical stenosis in IVUS. The addition of contrast QFR to % DS assessed by 2D QCA or %PV/RV assessed by 3D QCA also significantly improved the discrimination and reclassification of the anatomical stenosis lesion assessed by IVUS (AUC: from 0.787 to 0.881; NRI: 1.023, p <0.001; IDI: 0.196, p <0.001 in %DS assessed by 2D QCA and AUC: from 0.747 to 0.869; NRI: 1.002, p <0.001; IDI: 0.240, p <0.001 in %PV/RV assessed by 3D QCA) (**Table 10**).

The contrast QFR also improved the discrimination of the adverse plaque in IVUS. Although there was no significant difference in ROC comparison, the results of the NRI and IDI showed that the addition of contrast QFR to % DS assessed by 2D QCA or %PV/RV assessed by 3D QCA improved the discrimination and reclassification of adverse plaque characteristics assessed by IVUS (AUC: from 0.600 to 0.642; NRI: 3.332, p=0.002; IDI: 0.025, p=0.001 in %DS assessed by 2D

QCA and AUC: from 0.603 to 0.643; NRI: 0.362, p <0.001; IDI: 0.027, p <0.001 in %PV/RV assessed by 3D QCA) (**Table 10**).

Table 10. Incremental value of QFR over %diameter stenosis for assessing FFR ≤0.80

	AUC		Category free NRI		IDI	
	Value	**p value**	**Value**	**p value**	**Value**	**p value**
FFR ≤0.80						
% DS assessed by 2D QCA (reference)	0.742	<0.001				
% DS assessed by 2D QCA + contrast QFR	0.973	<0.001				
		<0.001*	1.663	<0.001	0.585	<0.001
%DS by 3D QCA (reference)	0.828	<0.001				
%DS by 3D QCA + contrast QFR	0.973	<0.001				
		<0.001*	1.561	<0.001	0.433	<0.001
Anatomical stenosis assessed by IVUS†						
%DS assessed by 2D QCA	0.787	<0.001				
%DS assessed by 2D QCA + contrast QFR	0.881	<0.001				
		<0.001*	1.023	<0.001	0.196	<0.001
%PV/RV assessed by 3D QCA	0.747	<0.001				
%PV/RV assessed by 3D QCA + contrast QFR	0.869	<0.001				
		<0.001*	1.002	<0.001	0.240	<0.001
Attenuation plaque or positive remodeling or plaque rupture						
%DS assessed by 2D QCA	0.600	0.001				
%DS assessed by 2D QCA + contrast QFR	0.642	<0.001				
		0.053*	3.332	0.002	0.025	0.001

%PV/RV assessed by 3D QCA	0.603	0.001				
%PV/RV assessed by 3D QCA + contrast QFR	0.643	<0.001				
		0.055*	0.362	<0.001	0.027	<0.001

*Comparison of two ROC curves

†IVUS anatomical stenosis: MLA ≤3mm^2 OR (MLA≤4mm^2 & PB ≥70%).

Abbreviations: AUC, area under the curve; DS, diameter stenosis; FFR, fractional flow reserve; IDI, integrated discrimination index; IVUS, intravascular ultrasound; MLA, minimum lumen area; NRI; net reclassification index; PV, plaque volume; QCA, quantitative coronary angiography; QFR, quantitative flow ratio; RV, reference volume.

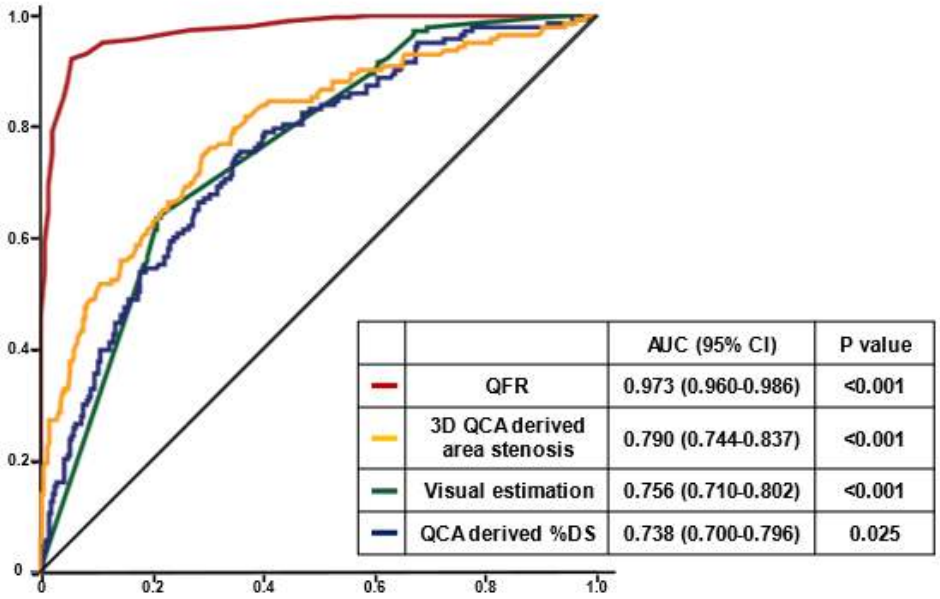

Figure 12. ROC curves for QFR, QCA-derived %DS, 3D QCA-derived area stenosis, and visual estimation for predicting FFR ≤0.80

Abbreviations: AUC, area under the receiver-operating characteristic curve; DS, diameter stenosis; FFR, fractional flow reserve; QCA, quantitative coronary angiography; QFR, quantitative flow ratio; ROC, receiver-operating curve.

Incremental value of QFR graph indices

The ischemia predictive ability of indicators obtained from QFR curves and 3D QCA was compared with QFR values. QFR graph indices, including $\%AAC_{lesion}$, and max angle, showed better diagnostic efficiency than 3D QCA data. However, the diagnostic efficacy of QFR was the best, and QFR alone seems sufficient to predict ischemia (AUC: 0.973; 95% CI: 0.959–0.986) (**Figure 13**). For adverse plaque (AP, PR, or rupture) prediction, QFR values, including contrast QFR, delta QFR, and graph index ($\%AAC_{lesion}$), showed better diagnostic efficiency than the anatomical indices obtained from the 3D QCA (**Figure 14**).

Although the diagnostic performance of QFR for predicting FFR ≤0.80 was good (accuracy 92.7%, sensitivity 91.7%, specificity 93.2%), there was an influence of lesion and disease subsets on the diagnostic performance of the QFR. There was no difference in accuracy for diabetes, ACS, or multiple lesions, but the accuracy decreased in vessels with diffuse disease (lesion length ≥35 mm) (**Figure 15**). Furthermore, the longer the length, the less accurate the QFR for FFR prediction. For vessels with lesion lengths over 35mm, the accuracy, sensitivity, and specificity of the QFR values were 78.8%, 84.2%, and 71.4%, respectively **(Table 11** and **Figure 16**). In diffuse disease, the addition of $\%AAC_{vessel}$ to contrast QFR demonstrated a tendency to improve the discrimination and reclassification of the vessels with FFR ≤0.80 (AUC: from 0.898 to 0.914; NRI: 0.886, p=0.011; IDI: 0.053, p=0.139) (**Table 12** and **Figure 17**).

Several indicators have been developed to predict residual ischemia. When residual ischemia after PCI was defined as post PCI QFR ≤0.92, the predictive values of QFR and %AAC were similar to those of the pullback pressure gradient

(PPG) index (p values for comparison, $\%AAC_{vessel}$ vs. PPG index: p=0.554, $\%AAC_{vessel}$ vs. QFR: p=0.328, PPG index vs. QFR: p=0.920) (**Figure 18**).

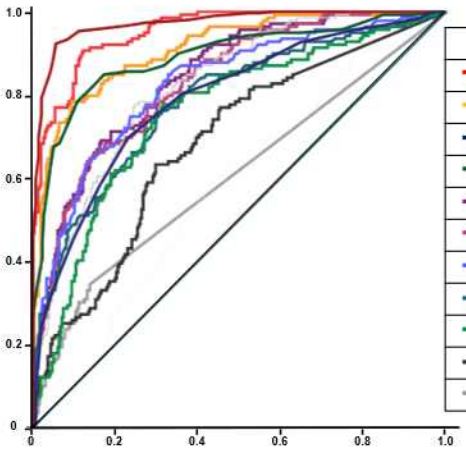

		AUC (95% CI)	P value
	QFR	0.973 (0.9590.986)	<0.001
	$Slope_{vessel}$	0.954 (0.9360.971)	<0.001
	$\%AAC_{lesion}$	0.911 (0.8820.940)	<0.001
	Delta QFR	0.893 (0.8570.929)	<0.001
	$Max\ angle_{vessel}$	0.843 (0.8050.881)	<0.001
	$Max\ angle_{lesion}$	0.833 (0.7930.872)	<0.001
	3D QCA derived %DS	0.826 (0.7840.869)	<0.001
	3D QCA derived %AS	0.786 (0.7380.833)	<0.001
	3D QCA %PV/RV	0.759 (0.7090.808)	<0.001
	$Angle_{lesion}$	0.686 (0.6320.739)	<0.001
	$Angle_{vessel}$	0.606 (0.5470.666)	<0.001

Figure 13. ROC curves for QFR curve data for predicting FFR ≤0.80

Abbreviations: AAC, area above the curve; AS, area stenosis; AUC, area under the receiver-operating characteristic curve; CI, confidence interval; DS, diameter stenosis; FFR, fractional flow reserve; PV, plaque volume; QCA, quantitative coronary angiography; QFR, quantitative flow ratio; RV, reference volume.

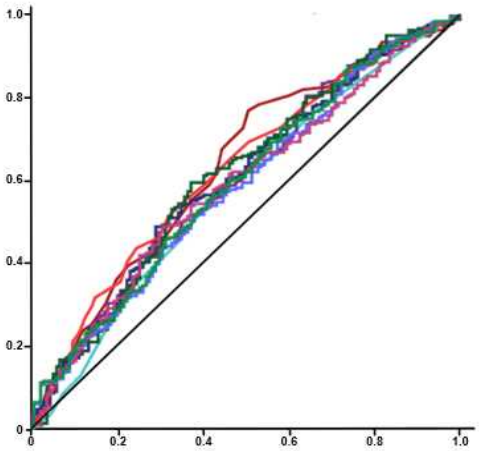

		AUC (95% CI)	P value
—	QFR	0.637 (0.5800.695)	<0.001
—	Delta QFR	0.624 (0.5660.683)	<0.001
—	$\%AAC_{lesion}$	0.611 (0.5510.671)	0.001
—	3D QCA %PV/RV	0.604 (0.5440.663)	0.001
—	3D QCA %DS	0.598 (0.5380.658)	0.002
—	$Max\ angle_{vessel}$	0.594 (0.5340.654)	0.003
—	$\%AAC_{vessel}$	0.588 (0.5280.647)	0.005
—	$Max\ angle_{lesion}$	0.583 (0.5230.643)	0.008
—	3D QCA MLD	0.577 (0.5170.636)	0.013

Figure 14. ROC curves for QFR curve data for predicting adverse plaque (AP, PR, or rupture)

Abbreviations: AAC, area above the curve; AP, attenuated plaque; AUC, area under the receiver-operating characteristic curve; DS, diameter stenosis; MLD, minimal lumen diameter; PR, positive remodeling; PV, plaque volume; QCA, quantitative coronary angiography; QFR, quantitative flow ratio; RV, reference volume.

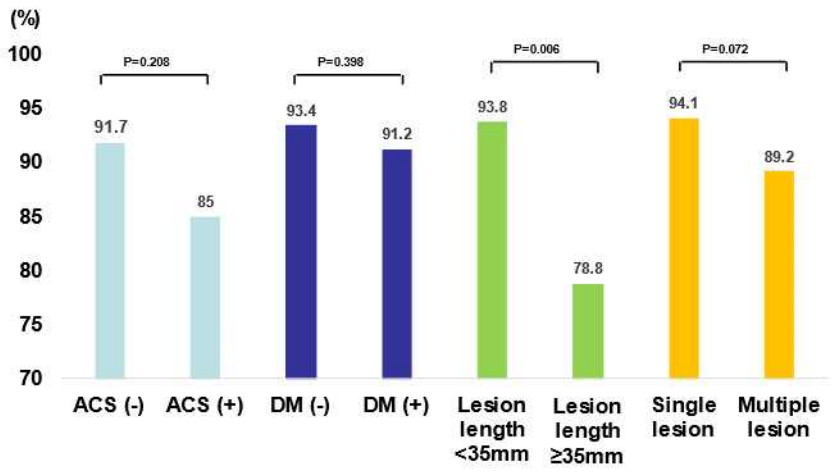

Figure 15. Influence of lesion and disease subsets on the diagnostic performance of the QFR

Abbreviations: ACS, acute coronary syndrome; DM, diabetes mellitus; QFR, quantitative flow ratio.

Table 11. Comparison of diagnostic performance of QFR for FFR ≤0.80 according to lesion length

	Total	Lesion length ≥30 mm (n=115)	Lesion length ≥35 mm (n=64)	Lesion length ≥40 mm (n=38)
True positive	132 (29.2)	27 (45.8)	16 (48.5)	11 (57.9)
True negative	287 (63.5)	22 (37.2)	10 (30.3)	3 (15.8)
False positive	21 (4.6)	5 (8.5)	4 (12.1)	3 (15.8)
False negative	12 (2.7)	5 (8.5)	3 (9.1)	2 (10.5)
Accuracy, %	92.7 (89.9-94.9)	83.1 (71.0-91.6)	78.8 (61.1-91.0)	73.7 (48.8-90.9)
Sensitivity, %	91.7 (85.9-95.6)	84.4 (67.2-94.7)	84.2 (60.4-96.6)	84.6 (54.6-98.1)
Specificity, %	93.2 (89.8-95.7)	81.5 (61.9-93.7)	71.4 (41.9-91.6)	50.0 (11.8-88.2)
Positive predictive value, %	86.3 (80.6-90.5)	84.4 (70.7-92.4)	80.0 (63.1-90.4)	78.6 (61.5-89.4)
Negative predictive value, %	96.0 (93.3-97.6)	81.5 (65.9-90.9)	76.9 (52.9-90.8)	60.0 (25.0-87.1)
Positive likelihood ratio	13.4 (8.9-20.4)	4.6 (2.0-10.2)	3.0 (1.3-6.9)	1.7 (0.7-3.9)
Negative likelihood ratio	0.09 (0.05-0.15)	0.19 (0.08-0.44)	0.22 (0.07-0.66)	0.31 (0.07-1.39)

Abbreviations: FFR, fractional flow reserve; QFR, quantitative flow ratio.

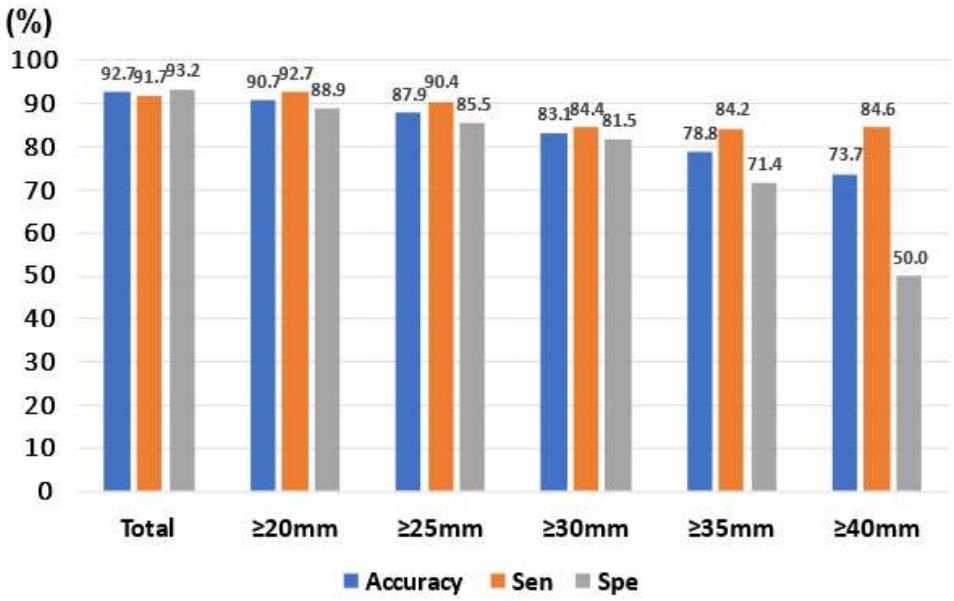

Figure 16. Diagnostic performance of QFR for FFR ≤0.80 according to lesion length

Abbreviations: FFR, fractional flow reserve; QFR, quantitative flow ratio.

Table 12. Incremental value of AAC over QFR for assessing FFR ≤0.80 in diffuse lesion (lesion length ≥35 mm)

	AUC		Category free NRI		IDI	
	Value	**p value**	**Value**	**p value**	**Value**	**p value**
FFR ≤0.80						
Contrast QFR	0.898	<0.001				
Contrast QFR + vessel %AAC	0.914	<0.001				
		0.389*	0.886	0.011	0.053	0.139

*Comparison of two ROC curves

Abbreviations: AAC, area above the curve; AUC, area under the curve; FFR, fractional flow reserve; IDI, integrated discrimination index; NRI; net reclassification index; QFR, quantitative flow ratio.

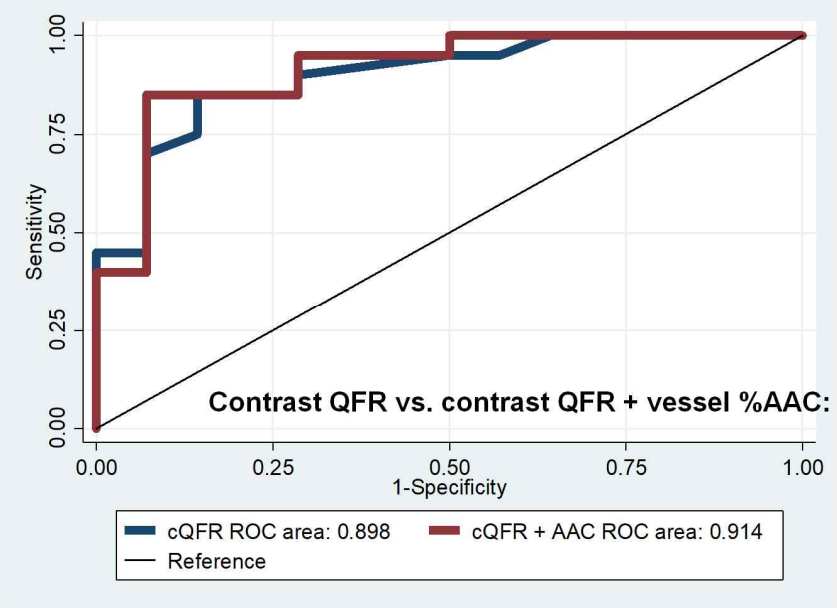

Figure 17. Incremental value of %AAC in vessels with diffuse disease (lesion length ≥35 mm)

Abbreviations: AAC, area above the curve; QFR, quantitative flow ratio; ROC, Receiver operating characteristic.

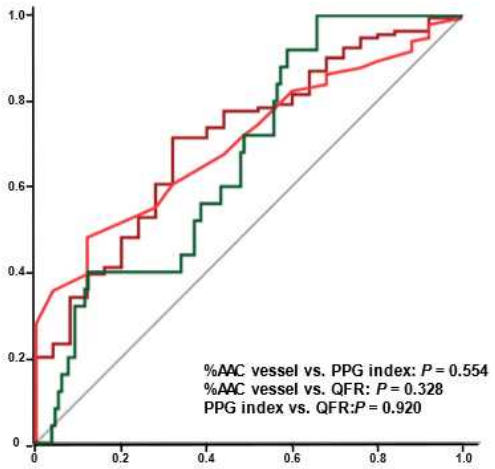

	AUC (95% CI)	P value
PPG index	0.712 (0.606-0.817)	0.001
QFR	0.704 (0.610-0.799)	0.001
%AAC $_{vessel}$	0.667 (0.565-0.770)	0.008

Figure 18. ROC curves for predicting post QFR ≤0.92

Abbreviations: AAC, area above the curve; AUC, area under the curve; PPG, pullback pressure gradient; QFR, quantitative flow ratio; ROC, Receiver operating characteristic.

Discussion

The current study evaluated the efficacy of QFR in predicting ischemia and adverse plaque characteristics. It also evaluated the correlation between QFR and IVUS findings in patients with intermediate coronary stenosis. The lower QFR (QFR ≤0.80) discriminated severe anatomical stenosis in IVUS and associated with the adverse plaque characteristic assessed by IVUS. Lower QFR was the independent predictor for adverse plaque. Furthermore, contrast QFR had an incremental value in discriminating FFR ≤0.80, anatomical stenosis assessed by IVUS, and adverse plaque characteristics. These findings suggested that QFR can predict ischemic lesions and plaque characteristics. A higher final QFR (≥0.92) value was associated with improved vessel outcomes. In diffuse disease (lesion length ≥35 mm), the accuracy of QFR in predicting FFR ≤0.80 decreased, and the addition of the QFR graph index may be helpful.

Invasive physiologic index

Evidence demonstrated that ischemia, rather than anatomical stenosis, is the most important target for coronary revascularization. FFR is an invasive physiologic index and has been regarded as a gold standard tool to detect ischemia-causing stenosis. (1, 32) Several studies have shown that PCI can be safely deferred if FFR is ≥0.75. The DEFER trial compared the PCI group to the deferral group in patients with intermediate stenosis. The result showed that PCI of a functionally nonsignificant stenosis (FFR ≥0.75) did not reduce the adverse events and was not associated with improved function. (12, 33) However, recent studies used an FFR

cut-off of 0.80. In the FAME study, FFR-guided PCI improved clinical outcomes (death or myocardial infarction) and cost savings compared with angiography-guided PCI for up to 2 years. (2) Long-term safety of FFR-guided PCI was confirmed, although long-term follow-up at 5 years showed no significant difference in composite outcomes. (3) Among patients with stable CAD with FFR ≤0.80, PCI with DES improved clinical outcome at 2 years compared to medical therapy alone, which was driven by a lower rate of urgent revascularization rate in the PCI group. (34) Although FFR is a useful tool, FFR must be measured during maximal and stable hyperemia, which is induced by intravenous adenosine or intracoronary nicorandil administration. Recently, resting indices have been developed from instantaneous wave-free ratio (iFR), which does not require using a hyperemic agent. Two large-randomized studies revealed comparable results between FFR- and iFR-guided PCI strategies. (35, 36) Recently, several diastolic resting indexes including resting full-cycle ratio (RFR), diastolic pressure ratio (dPR), and resting Pd/Pa developed, have shown excellent correlation and same diagnostic accuracy in predicting low FFR. (37-39) Consequently, both FFR and iFR-guided revascularization strategies are recommended as Class IA in guidelines. (1, 4)

Non-invasive quantitative flow ratio and invasive fractional flow reserve

Despite Class IA recommendations for FFR, the invasive pressure wire penetration rate is still low. Reasons for the low penetration rate of coronary physiology include procedural risk, prolonged procedure time, costs of hyperemic agents,

patient discomfort, challenges with repeatability, or physician experience. (5) To overcome these pitfalls, there have been several developments for calculating FFR non-invasively. Computational fluid dynamics (CFD) methods applied to coronary computed tomography (CT) angiography have enabled calculating FFR_{CT} without additional medication or imaging. FFR_{CT} showed a good correlation with FFR and good diagnostic performance in predicting ischemia (FFR ≤0.80) (Accuracy: 73% to 87%; Sensitivity: 82% to 93%; Specificity: 69% to 86%). (40-42) However, FFR_{CT} is expensive and time-consuming because CT images must be sent to an outside company. Another novel method is angiography-derived FFR. There are three major components to these methods: (i) 3D-QCA reconstruction from two 2-dimensional angiograms, (ii) estimation of flow or resistance to enable physiology input and (iii) addition of physiology data to the model via CFD principles or simple mathematic formulas. (43) Angiography-derived FFR is a novel approach to evaluate coronary physiology, based on the dedicated software non-invasively. QFR is the most validated angiography-derived FFR and calculated the pressure drop using a mathematical formula determined by stenosis geometry and mean hyperemic flow velocity. Mean hyperemic flow is calculated from the TIMI frame count in the patient's angiograms. QFR can be obtained through conventional CAG non-invasively and readily available during the diagnostic angiography procedure. Furthermore, QFR showed good agreement and diagnostic accuracy compared to FFR. (6, 44, 45) We also found a good direct correlation between QFR and FFR (Pearson's correlation coefficient: 0.75; $p < 0.001$). The diagnostic accuracy of QFR ≤0.80 for predicting FFR ≤0.80 was 92.7%. At lesions with a %DS 50%–70%, the variation in QFR values was wider than that of FFR. It might be an intrinsic

limitation of simulated indices that do not reflect collateral or microvascular dysfunction.

Other methods of angiography-derived FFR

Methods for calculating angiography-derived FFR are software-based methods. Most methods of angiography-derived FFR calculate the pressure ratio through CFD or simplified calculation formulas. There are several angiography-derived FFR methods using mathematical formulas. The QFR is one of the most well-known angiography-derived FFR methods using mathematical formulas. FFRangio (CathWorks) provides a 3D functional angiographic mapping of coronary trees with overlaid and color-coded FFR values. (46) The reconstruction is based on ≥3 projection angiograms and uses epipolar ray tracing with mathematical constraints to enhance the structure of the coronary tree. The coronary tree can be surfaced using a triangular mesh and rendered to display a 3D coronary tree model. Regarding hemodynamic evaluation, the resistance of a vessel can be estimated from the length and diameter, applying Poiseuille law, and neglecting entrance effects and peculiarities of rheology. FFR_{angio} provides multi-vessel FFR in a single analysis.

Most angiography-derived FFR methods rely on CFD. Inherited limitations of these methods may exist concerning generating theoretical boundary conditions to create a “one-size-fits-all”, and it takes too long computation time for flow simulations. Morris et al. used CFD-based angiography-derived FFR to overcome these shortcomings and showed clinical efficacy of vFFR (Virtual FFR) and high accuracy, but this system requires a rotational coronary angiogram and a long

processing time (up to 24 hours of computational time). (47) Virtual functional assessment index (vFAI) also showed a diagnostic performance to predict FFR. (48) 3D-QCA models were processed with CFD to calculate the pressure gradient (delta P) and draw the delta P-flow curve, then vFAI was derived from the delta P-flow curve. It only takes 15 minutes to calculate, but the blood flow was assumed, not a personalized boundary assessment. In addition, many angiography-derived FFR methods are being developed.

Values of QFR to predict IVUS findings

Although the lesions with anatomical stenosis assessed by IVUS had a lower QFR value, our study found that one-third of patients with IVUS anatomical stenosis had high QFR values, and 5.4% of lesions without IVUS anatomical stenosis had low QFR values. As seen in previous IVUS studies, it is rare to find QFR ≤0.80 with anatomical non-severe stenosis assessed by IVUS. The general revascularization criteria for MLA are so generous that the IVUS MLA-guided PCI could be associated with more false-positive outcomes than FFR-guided PCI. Thus, IVUS-guided PCI strategy may be associated with a higher PCI rate than the FFR-guided strategy, as seen in the FLAVOUR main study. Previous studies reported the relationships between the functional stenosis and parameters assessed by IVUS, including MLA, MLD, and plaque burden. (15, 23, 49) The FIRST prospective registry showed a moderate correlation of MLA with FFR values, with cut-off values for detecting significant hemodynamic stenosis (<2.4 mm^2, <2.7 mm^2, and <3.6 mm^2) dependent on reference vessel diameter (<3.0 mm, 3.0–3.5 mm, and >3.5 mm, respectively). The FIRST study showed that different MLA cut-offs

should be used to determine PCI, and FFR correlated with plaque burden but not plaque morphology seen in Virtual Histology-IVUS. (15) Although the relationship between the IVUS-derived plaque morphology and functional ischemia was not well known, recent studies with plaque morphology assessed by CT showed that lipid-rich plaques or PR are associated with ischemia irrespective of the degree of coronary stenosis. (50-53) Low-density non-calcified plaque indicates the presence of a necrotic core in coronary CT. Plaques with necrotic cores are rich in oxidative stress and inflammation. With an increase in oxidative stress, nitric oxide (NO) consumption decreases the bioavailability of NO and impairs the vasomotor function of the endothelium. (54, 55) Therefore, a relationship between the presence of large necrotic cores and ischemia is expected, but whether this was reflected in the QFR will require further studies. In another study with near-infrared spectroscopy (NIRS)-IVUS, QFR-positive lesions had a higher $maxLCBI_{4mm}$ compared to QFR-negative lesions. (56) Because NIRS detects lipids within plaques, this result demonstrated a relationship between lipid-rich plaques and ischemia. Interestingly, our study showed correlations between anatomical and various morphological IVUS characteristics and QFR values. It was confirmed that the IVUS-derived anatomical features, including MLA, MLD, and plaque burden, and the morphological features, including AP, PR, and plaque rupture, correlated with QFR values. Furthermore, QFR showed a high negative predictive value (97.5%) in plaques having AP and PR; it may function as a screening tool for high-risk plaque.

Influence of lesion and disease subsets on the diagnostic performance of the QFR

There was no difference in diagnostic accuracy of QFR for predicting FFR ≤0.80 in diabetes, ACS, or multiple lesions, but the accuracy decreased in vessels with diffuse disease (lesion length ≥35 mm). As the lesion length increased, the accuracy of QFR for predicting FFR ≤0.80 decreased. FFR also has limitations for diffuse lesions; interpreting the FFR results is challenging in patients with diffuse disease or multiple stenoses. In the case of multiple stenoses, stenosis influences the FFR of the others. Due to the second lesion, the FFR value of the first lesion can be underestimated. Similarly, the proximal lesions may overestimate the distal FFR values. (57) So, there have been studies on using FFR in diffuse or multiple diseases. In a study with 141 vessels with serial stenoses within the same coronary artery, coronary arteries were assessed by FFR with pullback pressure tracings. (58) The stenosis that caused the largest pressure step was stented first, and pullback pressure tracing was performed. Although this method is safe and useful for determining the proper target lesions for revascularization, repetitive pressure wire pullback should be performed. Pijls. et al. developed a complex formula to determine the FFR of individual stenosis when each stenosis is one of several in sequence. (59) However, coronary wedge pressure is essential for calculating the formula, which means that at least one percutaneous transluminal coronary angioplasty should be performed. That is, FFR values in diffuse or tandem disease are not as generalized as the prediction of a single lesion. These characteristics may have reduced the predictive power of QFR for FFR ≤0.80 in diffuse lesions. In another study, the diagnostic accuracy of QFR against FFR in vessels with tandem

lesions was lower than in those with single lesions. (60) In our study, the addition of $\%AAC_{vessel}$ to contrast QFR demonstrated a tendency to improve the discrimination and reclassification of the vessels with FFR ≤0.80. Due to the small number of vessels with diffuse disease, we could not find a significant difference, so larger studies are needed.

Relationship between final QFR and clinical outcome

FAVOR 3 China study showed that QFR-guided vessel and lesion selection strategy improved one-year clinical outcomes compared with standard angiography guidance in patients who underwent PCI (HR: 0.65; 95% CI: 0.51-0.83; p value <0.001). (12) Because PCI was performed in the low QFR group, there were no differences in clinical outcomes between the low and high QFR groups in our study. Also, baseline characteristics, including gender, target vessel, lesion location, and diagnosis, were worse in the low QFR group. However, we defined the final QFR value, the low final QFR (final QFR <0.92) group showed higher TVF incidence compared to the high final QFR group (final QFR ≥0.92) (HR: 3.21; 95% CI: 1.17–8.84; p=0.024). This finding is consistent with previous studies with post PCI FFR values. DEFINE PCI study showed that almost 25% of patients had residual ischemia despite angiographically successful PCI. (61) Reasons for residual ischemia include stent under-expansion, mal-apposition, edge dissection, or plaque protrusion. Accumulating evidence showed that residual ischemia is associated with a worse clinical outcome, and several studies have attempted to find optimal post PCI FFR value or optimal FFR gain. Nam et al. evaluated 80 patients who underwent FFR after PCI with DES and showed that the incidence of major

adverse cardiac event (MACE) at 1 year was higher in patients with post PCI FFR ≤0.90 compared with patients with post PCI FFR >0.90. (19) Another study by Doh et al. suggested post PCI FFR of 0.89 as a cut-off value, the high post PCI FFR (≥0.89) lesions had a better TVF-free survival rate compared with low post PCI FFR (<0.89) lesions. (62) In many other studies emphasizing the importance of FFR after PCI, the optimal cut-off value of post-PCI FFR varied from 0.86 to 0.96. (18, 63-65) In addition, a study showed the role of %FFR increase in evaluating the result of the PCI. (18) The relative increase of FFR was calculated by the percent difference of FFR before and after PCI ([post-PCI FFR - pre-PCI FFR]/pre-PCI FFR × 100) and named as %FFR increase (%FFR increase). (18) Patients with a low %FFR increase (≤15%) had a higher risk of TVF compared with those with a high %FFR increase. Adding the relative %FFR increase to post PCI FFR could enable better discrimination function for evaluating high-risk patients after PCI. However, the adoption of the post-PCI FFR rate is too low in real-world practice, so post-PCI QFR can be used as an alternative, demonstrating relevant clinical results. (66-67) The optimal cot-off values for QFR after PCI in other studies ranged from 0.89 to 0.92. Lower post-PCI QFR values (≤0.89) were independent predictors of adverse events in patients with chronic coronary syndromes or ACS. (67) In a total of 792 patients with ACS (49% STEMI and 51% NSTEMI), an optimal cut-off value of 0.89 for postinterventional culprit vessels and 0.85 for non-culprit vessels were determined as thresholds for the prediction of rates of MACE after ACS. (68) The theoretical benefits of QFR over other PCI optimization tools can be more broadly implemented in clinical practice. Also, adding a QFR index to QFR is a useful tool for post-PCI optimization. Because

disease patterns and local severity affect post PCI physiology, recent studies developed a PPG index to discriminate focal from diffuse disease. PPG index can be calculated by two parameters obtained from the FFR pullback curves; 1) $MaxPPG_{20mm}$: depicting the magnitude of FFR drop, and 2) the length of functional disease in which FFR deterioration. PPG index = {$MaxPPG_{20mm}$/ΔFFR + (1-Length with functional disease (mm)/Total vessel length (mm)}/2. (69) Because the PPG index quantifies the distribution of coronary disease and discriminates focal from diffuse disease, another study used a QFR-derived PPG index to show its effects on post-PCI physiologic results and clinical outcomes. (70) However, calculating the PPG index requires the slope of the pullback curve, and the formula is complex and not intuitive. In our study, when predicting low QFR values after PCI, QFR and %AAC showed similar predictive power to the PPG index. QFR and QFR graph index could be new metrics for predicting ischemia after PCI.

Clinical value of QFR

There are several limitations of the current study. First, because the FLAVOUR study was not originally intended for QFR analysis, the angiography was not acquired according to the specific acquisition protocol of QFR analysis. Therefore, only 47.6% of vessels were analyzable for QFR. Second, the criteria for PCI in our study did not reflect the local hemodynamic features and plaque vulnerability. Third, IVUS and FFR were not performed simultaneously in one patient, so ischemia was inferred from the QFR value. However, in the FFR group, we demonstrated a good correlation between QFR and FFR (Pearson's correlation coefficient: 0.75; $p < 0.001$). Fourth, the current study could not evaluate the

prognostic impact of the QFR since all patients underwent PCI based on pre-PCI FFR ≤0.80 or IVUS MLA ≤3mm^2 or MLA ≤4mm^2 & plaque burden ≥70%. Fifth, the distal part of the QFR analysis was arbitrarily located in the distal part of the vessel. Lastly, calculating QFR requires user interaction at steps such as angiogram selection, frame selection, lumen contouring, and contrast flow evaluation. But if the operator crosses the appropriate learning curve, the QFR result could be reliable. Standard operating procedures and observer training can reduce minor differences. As the software program is updated, the steps required by the operator are increasingly automated and simplified in a QFR (Medis Suite XA). Recent updates included improved contour detection, end-diastole detection by artificial intelligence, auto-corrected correspondence function, and enhanced automatic frame counting workflow (QFR® 2.1). In the future, it is necessary to standardize the evaluation method for fully automatic analysis using artificial intelligence.

Nevertheless, this less invasive angiography-derived FFR based on routine angiography that does not require a guiding catheter, pressure wire, and hyperemic agent, could be applied to real-world practice more easily, and less expensively in catheterization laboratories. Despite excellent correlation and diagnostic agreement of QFR and FFR, QFR analysis had a shorter measurement time than FFR. (44) In our study, the average calculation time of QFR was 7 minutes, and simple lesions were calculated in 3 minutes. The cost-effectiveness of QFR was explained in the QFR health technology assessment reported to the National Institute for Health Research. (71) For cost effectiveness, when a net benefit is expressed as a net health benefit (NHB), it is calculated by the quality-adjusted life-year (QALY) minus the cost/cost-effectiveness threshold. A cost-effectiveness threshold of

£20,000 per additional QALY was used in the analysis. In an interventional setting, the strategy with the highest NHB is strategy 2 (CAG followed by confirmatory FFR/iFR). However, the difference in net benefit between strategy two and the next best strategy (CAG with QFR using QAngio XA 3D/QFR) was relatively small (0.007 QALYs). But in diagnostic setting, CAG with QFR may result in a higher net benefit than strategy 1 (CAG only). The main factor of cost-effectiveness was the diagnostic sensitivity of QFR results. This is because 'true positive' means a higher QALY gain than mismanaging 'false-negative' results. We demonstrated that QFR was superior to 2D-QCA in ischemia assessment. Although we know that QFR cannot completely replace FFR, the indication of QFR can be extended to do a physiologic assessment when financial problems or the reimbursement system limits the use of pressure wires. Using the QFR-FFR hybrid approach (QFR-treat 0.77 and QFR-defer 0.86), a previous study showed that pressure wire and adenosine could be saved in 64% of all lesions. (44) Using QFR, we anticipate that CAG is no longer just a luminogram, but can provide comprehensive information that includes anatomical and physiological information and plaque characteristics to guide clinical decision-making. Through these benefits, angiography-derived FFR has the potential to change clinical practice in the future.

In conclusion, lower QFR (QFR ≤0.80) is related to IVUS-defined anatomical stenosis and associated with the adverse plaque characteristic assessed by IVUS. Furthermore, contrast QFR had an incremental value in discriminating FFR ≤0.80, anatomical stenosis assessed by IVUS, and adverse plaque characteristics. These findings suggested that QFR can predict ischemic lesions and plaque characteristics.

References

1. Neumann F-J, Sousa-Uva M, Ahlsson A, et al. 2018 ESC/EACTS Guidelines on myocardial revascularization. *Eur Heart J.* 2019;40(2):87-165.

2. Pijls NHJ, Fearon WF, Tonino PAL, et al. Fractional Flow Reserve Versus Angiography for Guiding Percutaneous Coronary Intervention in Patients With Multivessel Coronary Artery Disease. *J Am Coll Cardiol*. 2010;56(3):177-84.

3. van Nunen LX, Zimmermann FM, Tonino PA, et al. Fractional flow reserve versus angiography for guidance of PCI in patients with multivessel coronary artery disease (FAME): 5-year follow-up of a randomised controlled trial. *Lancet.* 2015;386(10006):1853-60.

4. Knuuti J, Wijns W, Saraste A, et al. 2019 ESC Guidelines for the diagnosis and management of chronic coronary syndromes. *Eur Heart J.* 2020;41(3):407-77.

5. Götberg M, Cook CM, Sen S, et al. The Evolving Future of Instantaneous Wave-Free Ratio and Fractional Flow Reserve. *J Am Coll Cardiol.* 2017;70(11):1379-402.

6. Xu B, Tu S, Qiao S, et al. Diagnostic Accuracy of Angiography-Based Quantitative Flow Ratio Measurements for Online Assessment of Coronary Stenosis. *J Am Coll Cardiol.* 2017;70(25):3077-87.

7. Westra J, Andersen BK, Campo G, et al. Diagnostic Performance of In-Procedure Angiography-Derived Quantitative Flow Reserve Compared to Pressure-Derived Fractional Flow Reserve: The FAVOR II Europe-Japan Study. *J Am Heart Assoc.* 2018;7(14):e009603.

8. Xu B, Tu S, Song L, et al. Angiographic quantitative flow ratio-guided coronary intervention (FAVOR III China): a multicentre, randomised, sham-controlled trial. *Lancet.* 2021;398(10317):2149-59.

9. Maehara A, Mintz GS, Bui AB, et al. Morphologic and angiographic features of coronary plaque rupture detected by intravascular ultrasound. *J Am Coll Cardiol.* 2002;40(5):904-10.

10. Endo M, Hibi K, Shimizu T, et al. Impact of ultrasound attenuation and plaque rupture as detected by intravascular ultrasound on the incidence of no-reflow phenomenon after percutaneous coronary intervention in ST-segment elevation myocardial infarction. *JACC Cardiovasc Interv.* 2010;3(5):540-9.

11. Wu X, Mintz GS, Xu K, et al. The relationship between attenuated plaque identified by intravascular ultrasound and no-reflow after stenting in acute myocardial infarction: the HORIZONS-AMI (Harmonizing Outcomes With Revascularization and Stents in Acute Myocardial Infarction) trial. *JACC Cardiovasc Interv.* 2011;4(5):495-502.

12. Bech GJ, De Bruyne B, Pijls NH, et al. Fractional flow reserve to determine the appropriateness of angioplasty in moderate coronary stenosis: a randomized trial. *Circulation.* 2001;103(24):2928-34.

13. Mintz GS, Guagliumi G. Intravascular imaging in coronary artery disease. *Lancet.* 2017;390(10096):793-809.

14. Buccheri S, Franchina G, Romano S, et al. Clinical Outcomes Following Intravascular Imaging-Guided Versus Coronary Angiography-Guided Percutaneous Coronary Intervention With Stent Implantation: A Systematic Review and Bayesian Network Meta-Analysis of 31 Studies and 17,882 Patients. *JACC Cardiovasc interv.* 2017;10(24):2488-98.

15. Waksman R, Legutko J, Singh J, et al. FIRST: Fractional Flow Reserve and Intravascular Ultrasound Relationship Study. *J Am Coll Cardiol.* 2013;61(9):917-23.

16. Park SJ, Ahn JM, Kang SJ, et al. Intravascular ultrasound-derived minimal lumen area criteria for functionally significant left main coronary artery stenosis. *JACC Cardiovasc interv.* 2014;7(8):868-74.

17. Stone GW, Maehara A, Lansky AJ, et al. A prospective natural-history study of coronary atherosclerosis. *N Engl J Med.* 2011;364(3):226-35.

18. Lee JM, Hwang D, Choi KH, et al. Prognostic Implications of Relative Increase and Final Fractional Flow Reserve in Patients With Stent Implantation. *JACC Cardiovasc Interv.* 2018;11(20):2099-109.

19. Nam CW, Hur SH, Cho YK, et al. Relation of fractional flow reserve after drug-eluting stent implantation to one-year outcomes. *Am J Cardiol.* 2011;107(12):1763-7.

20. Kang J, Koo B-K, Hu X, et al. Comparison of Fractional FLow Reserve And Intravascular ultrasound-guided Intervention Strategy for Clinical OUtcomes in Patients with InteRmediate Stenosis (FLAVOUR): Rationale and design of a randomized clinical trial. *Am Heart J.* 2018;199:7-12.

21. Suzuki N, Asano T, Nakazawa G, et al. Clinical expert consensus document on quantitative coronary angiography from the Japanese Association of Cardiovascular Intervention and Therapeutics. *Cardiovasc Interv Ther.* 2020;35(2):105-16.

22. Pijls NHJ, de Bruyne B, Peels K, et al. Measurement of fractional flow reserve to assess the functional severity of coronary-artery stenoses. *N Engl J Med.* 1996;334(26):1703-8.

23. Koo B-K, Yang H-M, Doh J-H, et al. Optimal Intravascular Ultrasound Criteria and Their Accuracy for Defining the Functional Significance of Intermediate Coronary Stenoses of Different Locations. *JACC Cardiovasc Interv.* 2011;4(7):803-11.

24. Pijls NH, van Son JA, Kirkeeide RL, et al. Experimental basis of determining maximum coronary, myocardial, and collateral blood flow by pressure measurements for assessing functional stenosis severity before

and after percutaneous transluminal coronary angioplasty. *Circulation.* 1993;87(4):1354-67.

25. Mintz GS, Nissen SE, Anderson WD, et al. American College of Cardiology Clinical Expert Consensus Document on Standards for Acquisition, Measurement and Reporting of Intravascular Ultrasound Studies (IVUS). A report of the American College of Cardiology Task Force on Clinical Expert Consensus Documents. *J Am Coll Cardiol.* 2001;37(5):1478-92.

26. Pu J, Mintz GS, Brilakis ES, et al. In vivo characterization of coronary plaques: novel findings from comparing greyscale and virtual histology intravascular ultrasound and near-infrared spectroscopy. *Eur Heart J.* 2012;33(3):372-83.

27. Kimura S, Kakuta T, Yonetsu T, et al. Clinical significance of echo signal attenuation on intravascular ultrasound in patients with coronary artery disease. *Circ Cardiovasc Interv.* 2009;2(5):444-54.

28. Kearney P, Erbel R, Rupprecht HJ, et al. Differences in the morphology of unstable and stable coronary lesions and their impact on the mechanisms of angioplasty. An in vivo study with intravascular ultrasound. *Eur Heart J.* 1996;17(5):721-30.

29. Fujii K, Kobayashi Y, Mintz GS, et al. Intravascular ultrasound assessment of ulcerated ruptured plaques: a comparison of culprit and nonculprit lesions of patients with acute coronary syndromes and lesions in patients without acute coronary syndromes. *Circulation.* 2003;108(20):2473-8.

30. Garcia-Garcia HM, McFadden EP, Farb A, et al. Standardized end point definitions for coronary intervention trials: the Academic Research Consortium-2 consensus document. *Eur Heart J.* 2018;39(23):2192-207.

31. DeLong ER, DeLong DM, Clarke-Pearson DL. Comparing the areas under two or more correlated receiver operating characteristic curves: a nonparametric approach. *Biometrics.* 1988;44(3):837-45.

32. Xaplanteris P, Fournier S, Pijls NHJ, et al. Five-Year Outcomes with PCI Guided by Fractional Flow Reserve. *N Engl J Med.* 2018;379(3):250-9.

33. Pijls NH, van Schaardenburgh P, Manoharan G, et al. Percutaneous coronary intervention of functionally nonsignificant stenosis: 5-year follow-up of the DEFER Study. *J Am Coll Cardiol.* 2007;49(21):2105-11.

34. De Bruyne B, Fearon WF, Pijls NH, et al. Fractional flow reserve-guided PCI for stable coronary artery disease. *N Engl J Med.* 2014;371(13):1208-17.

35. Davies JE, Sen S, Dehbi HM, et al. Use of the Instantaneous Wave-free Ratio or Fractional Flow Reserve in PCI. *N Engl J Med.* 2017;376(19):1824-34.

36. Götberg M, Christiansen EH, Gudmundsdottir IJ, et al. Instantaneous Wave-free Ratio versus Fractional Flow Reserve to Guide PCI. *N Engl J Med.* 2017;376(19):1813-23.

37. Lee JM, Choi KH, Park J, et al. Physiological and Clinical Assessment of Resting Physiological Indexes. *Circulation.* 2019;139(7):889-900.

38. van't Veer M, Pijls NHJ, Hennigan B, et al. Comparison of Different Diastolic Resting Indexes to iFR: Are They All Equal? *J Am Coll Cardiol.* 2017;70(25):3088-96.

39. Sen S, Escaned J, Malik IS, et al. Development and Validation of a New Adenosine-Independent Index of Stenosis Severity From coronary wave-intensity analysis: results of the ADVISE (ADenosine Vasodilator Independent Stenosis Evaluation) study. *J Am Coll Cardiol.* 2012;59(15):1392-402.

40. Koo BK, Erglis A, Doh JH, et al. Diagnosis of ischemia-causing coronary stenoses by noninvasive fractional flow reserve computed from coronary computed tomographic angiograms. Results from the prospective multicenter DISCOVER-FLOW (Diagnosis of Ischemia-Causing Stenoses Obtained Via Noninvasive Fractional Flow Reserve) study. *J Am Coll Cardiol.* 2011;58(19):1989-97.

41. Min JK, Leipsic J, Pencina MJ, et al. Diagnostic Accuracy of Fractional Flow Reserve From Anatomic CT Angiography. JAMA. 2012;308(12):1237-45.

42. Nørgaard BL, Leipsic J, Gaur S, et al. Diagnostic performance of noninvasive fractional flow reserve derived from coronary computed tomography angiography in suspected coronary artery disease: the NXT trial (Analysis of Coronary Blood Flow Using CT Angiography: Next Steps). *J Am Coll Cardiol.* 2014;63(12):1145-55.

43. Wong CCY, Yong ASC. Flash-forward: the emergence of angiography-derived fractional flow reserve in the catheter laboratory. *Cardiovasc Res.* 2020;116(7):1242-5.

44. Westra J, Andersen BK, Campo G, et al. Diagnostic Performance of In-Procedure Angiography-Derived Quantitative Flow Reserve Compared to Pressure-Derived Fractional Flow Reserve: The FAVOR II Europe-Japan Study. *J Am Heart Assoc.* 2018;7(14):e009603.

45. Tu S, Westra J, Yang J, von Birgelen C, et al. Diagnostic Accuracy of Fast Computational Approaches to Derive Fractional Flow Reserve From Diagnostic Coronary Angiography: The International Multicenter FAVOR Pilot Study. *JACC Cardiovas interv.* 2016;9(19):2024-35.

46. Pellicano M, Lavi I, De Bruyne B, et al. Validation Study of Image-Based Fractional Flow Reserve During Coronary Angiography. *Circ Cardiovasc Interv.* 2017;10(9):e005259.

47. Morris PD, Ryan D, Morton AC, et al. Virtual fractional flow reserve from coronary angiography: modeling the significance of coronary lesions: results from the VIRTU-1 (VIRTUal Fractional Flow Reserve From Coronary Angiography) study. *JACC Cardiovasc Interv.* 2013;6(2):149-57.

48. Papafaklis MI, Muramatsu T, Ishibashi Y, et al. Fast virtual functional assessment of intermediate coronary lesions using routine angiographic data and blood flow simulation in humans: comparison with pressure wire - fractional flow reserve. *EuroIntervention.* 2014;10(5):574-83.

49. Kang SJ, Lee JY, Ahn JM, et al. Validation of intravascular ultrasound-derived parameters with fractional flow reserve for assessment of coronary stenosis severity. *Circ Cardiovasc Interv.* 2011;4(1):65-71.

50. Driessen RS, Stuijfzand WJ, Raijmakers PG, et al. Effect of Plaque Burden and Morphology on Myocardial Blood Flow and Fractional Flow Reserve. *J Am Coll Cardiol.* 2018;71(5):499-509.

51. Driessen RS, de Waard GA, Stuijfzand WJ, et al. Adverse Plaque Characteristics Relate More Strongly With Hyperemic Fractional Flow Reserve and Instantaneous Wave-Free Ratio Than With Resting Instantaneous Wave-Free Ratio. *JACC Cardiovasc Imaging.* 2020;13(3):746-56.

52. Park H-B, Heo R, Ó Hartaigh B, et al. Atherosclerotic plaque characteristics by CT angiography identify coronary lesions that cause ischemia: a direct comparison to fractional flow reserve. *JACC Cardiovasc Imaging.* 2015;8(1):1-10.

53. Gaur S, Øvrehus KA, Dey D, et al. Coronary plaque quantification and fractional flow reserve by coronary computed tomography angiography identify ischaemia-causing lesions. *Eur Heart J.* 2016;37(15):1220-7.

54. Ahmadi A, Kini A, Narula J. Discordance between ischemia and stenosis, or PINSS and NIPSS: are we ready for new vocabulary? *JACC Cardiovasc Imaging.* 2015;8(1):111-4.

55. Ahmadi A, Stone GW, Leipsic J, et al. Association of Coronary Stenosis and Plaque Morphology With Fractional Flow Reserve and Outcomes. *JAMA Cardiol.* 2016;1(3):350-7.

56. Dobrolińska MM, Gąsior PM, Pociask E, et al. Performance of Integrated Near-Infrared Spectroscopy and Intravascular Ultrasound (NIRS-IVUS) System against Quantitative Flow Ratio (QFR). *Diagnostics (Basel).* 2021;11(7):1148.

57. Nijjer SS, Sen S, Petraco R, et al. The Instantaneous wave-Free Ratio (iFR) pullback: a novel innovation using baseline physiology to optimise coronary angioplasty in tandem lesions. *Cardiovasc Revasc Med.* 2015;16(3):167-71.

58. Kim HL, Koo BK, Nam CW, et al. Clinical and physiological outcomes of fractional flow reserve-guided percutaneous coronary intervention in patients with serial stenoses within one coronary artery. *JACC Cardiovasc Interv.* 2012;5(10):1013-8.

59. Pijls NHJ, Bruyne BD, Bech GJW, et al. Coronary pressure measurement to assess the hemodynamic significance of serial stenoses within one coronary artery: validation in humans. *Circulation.* 2000;102(19):2371-7.

60. Lee KY, Hwang BH, Kim MJ, et al. Influence of lesion and disease subsets on the diagnostic performance of the quantitative flow ratio in real-world patients. *Sci Rep.* 2021;11(1):2995.

61. Jeremias A, Davies JE, Maehara A, et al. Blinded Physiological Assessment of Residual Ischemia After Successful Angiographic Percutaneous Coronary Intervention: The DEFINE PCI Study. *JACC Cardiovasc Interv.* 2019;12(20):1991-2001.

62. Doh JH, Nam CW, Koo BK, et al. Clinical Relevance of Poststent Fractional Flow Reserve After Drug-Eluting Stent Implantation. J Invasive Cardiol. 2015;27(8):346-51.

63. Agarwal SK, Kasula S, Hacioglu Y, et al. Utilizing Post-Intervention Fractional Flow Reserve to Optimize Acute Results and the Relationship to Long-Term Outcomes. *JACC Cardiovasc Interv.* 2016;9(10):1022-31.

64. Nishi T, Piroth Z, De Bruyne B, et al. Fractional Flow Reserve and Quality-of-Life Improvement After Percutaneous Coronary Intervention in Patients With Stable Coronary Artery Disease. *Circulation.* 2018;138(17):1797-804.

65. Piroth Z, Toth GG, Tonino PAL, et al. Prognostic Value of Fractional Flow Reserve Measured Immediately After Drug-Eluting Stent Implantation. *Circ Cardiovasc Interv.* 2017;10(8):e005233.

66. Kogame N, Takahashi K, Tomaniak M, et al. Clinical Implication of Quantitative Flow Ratio After Percutaneous Coronary Intervention for 3-Vessel Disease. *JACC Cardiovasc Interv.* 2019;12(20):2064-75.

67. Biscaglia S, Tebaldi M, Brugaletta S, et al. Prognostic Value of QFR Measured Immediately After Successful Stent Implantation: The

International Multicenter Prospective HAWKEYE Study. *JACC Cardiovasc Interv.* 2019;12(20):2079-88.

68. Erbay A, Penzel L, Abdelwahed YS, et al. Prognostic Impact of Pancoronary Quantitative Flow Ratio Assessment in Patients Undergoing Percutaneous Coronary Intervention for Acute Coronary Syndromes. *Circ Cardiovasc Interv.* 2021;14(12):e010698.

69. Collet C, Sonck J, Vandeloo B, et al. Measurement of Hyperemic Pullback Pressure Gradients to Characterize Patterns of Coronary Atherosclerosis. *J Am Coll Cardiol.* 2019;74(14):1772-84.

70. Shin D, Dai N, Lee SH, et al. Physiological Distribution and Local Severity of Coronary Artery Disease and Outcomes After Percutaneous Coronary Intervention. *JACC Cardiovasc Interv.* 2021;14(16):1771-85.

71. Duarte A, Llewellyn A, Walker R, et al. Non-invasive imaging software to assess the functional significance of coronary stenoses: a systematic review and economic evaluation. *Health Technol Assess.* 2021;25(56):1-230.

국문 초록

서론: 심장혈관의 협착을 평가하고 중재 시술을 하는 가장 표준적인 평가 방법은 경피적 관상동맥 조영술이다. 관상 동맥 질환의 예후를 결정하는 가장 중요한 요소는 심근의 허혈 정도이며 이는 심근분획혈류 (fractional flow reserve, FFR)를 통해 확인할 수 있기에, FFR 을 이용한 재관류 시술이 중등도의 혈관 협착이 있는 환자에서 표준 치료로 알려져 있다. 하지만 FFR 측정은 시술 시간이 길어지고, 충혈제를 사용해야 하고, 압력 철선을 사용하는 불편함이 있다. 혈관 조영술 기반 정량적 유량비 (Quantitative flow ratio, QFR)는 컴퓨터 유체역학 기술을 기반으로 하여 2 개의 관동맥 조영술 영상을 가지고 관상동맥을 3 차원 재건하고 혈류의 속도에 대한 정보를 더하여 기존에 침습적으로만 얻어낼 수 있었던 FFR 의 값을 심혈관 조영술 영상만으로 구현해 내는 인공지능기술이다. 혈관내 초음파는 관상동맥 중재시술 하는 중에, 해부학적인 혈관 내 병변, 혈관 내 동맥경화반의 특성을 얻어낼 수 있는 도구이다. 이는 역시 침습적인 관동맥 중재술로 얻을 수 있는 정보이다. 아직 QFR 정보와 혈관내 초음파 정보와의 관계는 잘 알려진 바가 없어, 비침습적 QFR 값과 혈관내 초음파 정보사이의 관계에 대해 알아보고자 한다. 뿐만 아니라 우리는 QFR 을 구할 때 같이 얻을 수 있는 QFR 그래프에서 얻어낼 수 있는 인덱스로 환자에 있어 허혈과의 관계와 환자의 임상적 결과 사이의 관계도 확인하고자 한다.

방법: 기존의 전향적 연구인 FLAVOUR study 는 1700 명의 중등도 관상동맥 협착을 가진 환자들을 대상으로 무작위 배정하여 혈관내 초음파 기반의 관상동맥 중재술과 FFR 기반 관상동맥 중재술의 2 년 추적검사 결과를 바탕으로 하는 다기관, 전향적, 무작위 배정 임상 시험이다. 이 연구에 등록된 심혈관 조영술 중에 QFR 분석이 가능한 혈관을 검토하여 중앙 분석기관에서 QFR 분석을 시행하였다. QFR 값이 0.80 이하인 것을 혈역학적으로 유의미한 것으로 정의하였다. 혈관내 초음파 특성은 QFR 값 0.80 기준으로 두그룹간 비교하였다. Final QFR 의 의미는 중재술을 하지 않은 환자에서는 진단적 관상동맥 조영술 영상에서 계산한 QFR 값, 중재술을 시행한 환자는 시술 후 마지막 관상동맥 조영술 영상에서 얻은 QFR 값을 뜻한다. QFR 곡선 분석을 통해서 곡선 상방의 면적의 비율 (%area above the QFR curve, %AAC) 가 구해졌고 이는 곡선 위 면적/전체 면적 X 100 (%)으로 계산된다. 주가 되는 비교는 2 차원적 정량적 관상동맥 조영술 (2D-quantitative coronary angiography, 2D-QCA)에서 확인되는 직경 협착에 비해 QFR 0.80 이하가 FFR 0.80 이하를 예측하는 정확성으로 하였고, 기존 2D-QCA 에서 얻은 직경 협착에 비해 QFR 의 FFR 0.80 이하를 예측하는 Receiver Operating Characteristic Curve (ROC) 곡선의 면적 비교를 하였다. 혈관내 초음파군에서도 비슷한 방식으로 혈관내 초음파상의 해부학적인 협착, 불안정 동맥경화반을 예측하는 능력을 비교하였다. 일차 임상종료점은 2 년째 까지의 사망, 목표혈관 관련 심근경색, 목표혈관 재개통술로 정의하였다.

결과: 최종적으로 QFR 분석이 가능한 혈관은 867 개였다. 3D-QCA 직경 협착 50% 이상이 허혈을 예측하는 정확도는 52.2% 인 것에 비해,

QFR 0.80 이하의 허혈 예측 정확도는 92.7% 였다. QFR 의 FFR 0.80 이하를 예측하는 능력은 ROC 커브를 볼 때 2D-QCA 에서 얻어진 데이터나, 3D-QCA 에서 얻어진 데이터에 비해 AUC 면적이 컸다 (QFR: 0.973 vs. 2D QCA %DS: 0.738). QFR 0.80 이하인 군은 QFR 0.80 을 초과하는 군에 비해 병변의 길이가 길고, 최소 내강 면적은 작고, 동맥경화반의 양이 많았다. 해부학적인 특성뿐만 아니라, 동맥경화반의 특성도 차이가 있었는데, QFR 0.80 이하인 군은 QFR 0.80 을 초과하는 군에 비해 저음영 동맥경화반, 혼합 동맥경화반, 동맥경화반의 파열, 석회화 결절 및 양성 재형성의 비율이 높았고, 섬유성 동맥경화반의 비율은 낮았다. 다만 QFR 의 정확도는 목표병변의 길이가 35 mm 이상으로 길어질 경우에 감소하는 경향을 보였다. 이런 미만성 병변에서 QFR 에 $\%AAC_{vessel}$ 데이터를 추가할 경우에 FFR 0.80 이하를 예측하는 예측능이 호전되는 것을 확인하였다 (AUC: from 0.898 to 0.914; NRI: 0.886, p=0.011; IDI: 0.053, p=0.139). Final QFR 이 낮은 (<0.92) 군은 Final QFR 이 높은 군 (≥0.92)에 비해 일차 임상종료점 발생의 빈도가 높은 것을 확인할 수 있었다 (final QFR 낮은 군 vs. final QFR 높은 군: 4.7% vs. 1.5%; HR: 3.21; 95% CI: 1.17-8.84; p=0.017).

결론: QFR 0.80 이하인 군은 혈관내 초음파상 보이는 해부학적으로 심한 병변의 특성뿐 아니라, 혈관내 초음파상 확인되는 동맥경화반의 질적으로 나쁜 특성과도 관련이 있었다. QFR 데이터를 해부학적인 데이터에 추가하는 것은 혈관내 초음파상 해부학적인 협착 외에, 불리한 동맥경화반의 특성을 예측하는 데에 증분 가치가 있음을 확인하였다.

이것은 QFR 은 허혈뿐 아니라 동맥경화반의 나쁜 모양까지 예측하는 예측력이 있음을 뜻하는 것이다.

주요어: 심혈관 조영술을 통해 유추한 분획 혈류 예비력; 혈관 조영술 기반 정량적 유량비; 분획 혈류 예비력; 혈관내 초음파; 불리한 동맥경화반.

학번: 2020-35833